Copper dependent defects in mitochondria
by

Bre'Ida J. Riddick

A thesis submitted to the Graduate Faculty of
Auburn University
in partial fulfillment of the
requirements for the Degree of
Master of Science

Auburn, Alabama
August 7, 2021

Key words: Copper, heme biosynthesis, oxidative stress, protein thiols, Wilson disease

Approved by

Paul A. Cobine, Chair, Professor of Biological Sciences
Anthony G. Moss, Associate Professor of Biological Sciences
Alexey Petrov, Assistant Professor of Biological Sciences

Abstract

Wilson disease (WD) is a disease characterized by excessive copper accumulation in the liver and various other organs. Consequently, the excess copper deposits in these organs eventually cause damage to them. In WD copper is absorbed through dietary consumption and not properly excreted from the body. Excessive accumulation of copper leads to many negative clinical symptoms such as acute liver failure or cirrhosis. The copper accumulation leads to cellular damage and mitochondrial injury. Mitochondria are a direct target of copper ion damage due to mitochondria accumulating copper required for electron transport processes. Though we have identified who, or rather what, is affected by excess copper accumulation "why" and "how" remained unanswered. Little is known about the import and export of mitochondrial copper or proteins and mechanisms involved in copper dependent damage response. Described in this study are two copper dependent reactions:

1. The oxidation of cellular and mitochondrial thiols as a result of copper accumulation.
2. A copper related heme defect in *Saccharomyces cerevisiae* that is alleviated upon the deletion of *MRS3*.

Protein thiols are biologically significant and contribute to stable tertiary and quaternary protein structures. Oxidation of the thiol groups can lead to modulation of protein structure and subsequent negative impacts on protein function. Unbound copper ions are thought to damage protein thiols by causing the emergence of reactive oxygen species (ROS). These ROS can damage the mitochondria by causing structural damage and by inhibiting biochemical reactions. Herein we explore and demonstrate copper dependent damage that occurs in the cell due to sulfhydryl groups and observe a dose dependent decrease in total cellular thiols.

Heme is a critical iron cofactor in aerobic life that is synthesized primarily in mitochondria. Disturbed heme metabolism causes mitochondrial decay, oxidative stress, and iron accumulation. However before now there has not been a correlation drawn between imbalanced copper homeostasis and disrupted heme synthesis. A dose dependent heme defect in response to elevated exogenous copper was observed in yeast and this defect was alleviated by the deletion of *MRS3*. Taking this into account, the data presented does further solidify a role for iron transporter *MRS3* in copper import into mitochondrial matrix plus heme biosynthesis. The transport of both copper and iron by *MRS3* can lead to competition in high copper levels that results in alternative transport of iron meaning it is not being transported directly to the heme biogenesis proteins that are in a complex with Mrs3 thus disrupting heme biogenesis. Copper dependent defects in mitochondria prove to be an area that needs further investigation. Outlining these defects can help to identify more potential pathways and proteins involved in copper homeostasis to better understand mitochondrial metal metabolism.

Acknowledgments

Thank you to the people who all contributed to me completing my thesis here at Auburn University:

Dr. Paul Cobine who has been a great teacher and mentor. He has always offered advice, insight, and humor. I am grateful for the time I spent under his mentorship.

My committee, Dr. Anthony Moss and Dr. Alexey Petrov, who graciously agreed to contribute their time and expertise to me and my work.

Members of the Cobine Lab for VERY helpful guidance, comments, and suggestions.

Staff of the graduate school of the department of biological sciences for their patience and support.

Sydney V. Bell and Nitish Kunte for friendship, laughter and sometimes a much-needed pat on the back. I will always cherish the time we spent in Auburn.

To my parents Kerry and Shirelle Riddick, big brother Ryan Livingston and his clan, and other family members thank you for all your motivation and unconditional support! You all are always my motivation.

Table of Contents

List of Tables

List of Figures

List of Abbreviations

ATP	Adenosine Triphosphate
Ca^{2+}	Calcium (II) ion
COX	Cytochrome C oxidase
CHO	Chinese Hamster Ovary
CuHis	Copper histidine
$CuSO_4$	Copper sulfate
DHE	Dihydroethidium
FBS	Fetal Bovine Serum
Fe-S	Iron-sulfur
$FeSO_4$	Ferrous Sulfate
GSH	Glutathione
HEK 293	Human Embryonic Kidney 293
HPLC	High pressure liquid chromatography
IMM/IM	Inner mitochondrial membrane
MDH	Malate Dehydrogenase
OMM/OM	Outer mitochondrial membrane
PPIX	Protoporphyrin IX
ROS	Reactive oxygen species
WD	Wilson disease
$\Delta\Psi m$	Mitochondrial membrane potential

Chapter 1
Literature Review

1.1 Cell Biology Overview

Here we present a brief overview of major organelles of the eukaryotic cell. Organelles discussed in this chapter are relevant to understanding the context of this work. In future chapters we will examine the roles that some of the mentioned organelles play in the response of eukaryotic cells to dysfunction, specifically during copper overload.

The Plasma Membrane

The plasma membrane consists of both lipids and proteins [3]. The plasma membrane is the boundary of the cell that serves to maintain internal homeostasis of the cell, by acting to mediate entry and exit of substances to and from the cell. A major recognizable component of the plasma membrane is the phospholipid bilayer. Phospholipids contain both hydrophobic and hydrophilic regions which help the lipid bilayer serve as a barrier between two aqueous compartments.

While lipids are the building blocks for structure of the membrane of a cell, proteins are the key to proper cellular function. Membrane associated proteins can be separated into two classes: peripheral membrane proteins and integral membrane proteins. Integral membrane proteins are inserted into the lipid bilayer and many of them are identified as transmembrane proteins, meaning they are positioned so that parts of the protein are exposed on both sides of the plasma membrane [3]. In addition, both phospholipids and proteins diffuse laterally within the membrane [3]. Peripheral membrane proteins are associated with membranes through protein-protein interaction by ionic bonding [3].

Both integral and peripheral classes of proteins are involved in functions that are important to survival of organisms such as: cell signaling, transportation of molecules and ions

across the membrane, oxidoreductase activity, transferase activity, hydrolase activity or cell adhesion for cell-cell interaction [4,5]

Cell Wall

Bacteria and fungi both have a dual membrane system where the plasma membrane or cytoplasmic membrane is surrounded by a cell wall. The cell wall is composed of an outer layer which features heavily glycosylated mannoproteins projecting from the cell surface [6,7]. This cell well serves as an extra barrier, by limiting the accessibility of the inner part of the wall and the plasma membrane to foreign enzymes [8]. Fungi, plant, and bacterial cell walls both share a surface component with β1,4- and β1,3-linked polysaccharides as fibrous components. These glycans form ribbon-like or helical structures, as cellulose and chitin or β1,3 glucan respectively, to maintain the integrity of the cell wall. Characteristics of the cell wall can vary between organisms. Bacterial cell walls are cross-linked by peptides in comparison to plant cell walls that have cross-linking phenolics and polysaccharides. [9,10]

Mitochondria

Most eukaryotic cells contain numerous mitochondria, which can occupy up to 20 percent of the cytoplasm's volume [1]. Mitochondria are the main sites of Adenosine triphosphate (ATP) production during aerobic metabolism. Structurally, mitochondria are composed of an outer membrane (OMM) and inner membrane (IMM) separated by an intermembrane space (IMS) and the matrix compartment. The most permeable membrane is the OMM which has approximately 50 percent of lipids in its composition and allows exchange of small molecules with the cytoplasm but excludes proteins from entering the IMS. The IMM has nearly 30 percent less of lipids in its composition in comparison and has a higher proportion of

protein than other cellular membranes. This membrane is highly selective and sealed to allow for the generation of proton motive force. The surface area of the IMM is increased by infoldings, or cristae, that surround the matrix [1].

Energy Production in mitochondria

Generally, ATP synthesis via aerobic respiration occurs when glucose is oxidized to carbon dioxide CO_2 and the recycling of redox equivalents generates ATP. The process is usually expressed as the equation: $C_6H_{12}O_6$ [glucose] + $6O_2$ [oxygen] = ~38 ATP + $6CO_2$ [carbon dioxide] + $6H_2O$ [water]. In detail this equation summarizes and involves complex processes and pathways known as cellular respiration.

The first stage known is glycolysis, starts with glucose being metabolized into pyruvate in the cytoplasm of the cell. If mitochondrial function is blocked or disabled or an electron acceptor such as O_2 is not available (i.e., anaerobic conditions) the pyruvate is converted into lactic acid instead of CO_2 [2]. If mitochondrial function is operating under optimal conditions, after glycolysis pyruvate is broken down to create three molecules acetyl coenzyme A (acetyl-CoA), CO_2 and nicotinamide adenine dinucleotide (NAD) + hydrogen (H) (NADH).

Acetyl-CoA, a two-carbon molecule attached to coenzyme-A, goes into a cyclic pathway known as the Krebs cycle or tricarboxylic acid (TCA) cycle in the matrix of mitochondria. Acetyl-CoA is oxidized to form CO_2 and H_2O, from this reaction protons are distributed to proton carriers such as NAD+ and flavin adenine dinucleotide (FAD). These carriers are known as NADH and $FADH_2$ and are in their reduced state [2]. In their reduced state NADH and $FADH_2$ then enter the electron transport chain (ETC) at the mitochondrial inner membrane and in the cristae. The ETC is made up of a series of proteins called Complexes I–IV, that carry electrons along in a

designated sequence. In the beginning of the ETC, two electrons are released from NADH into Complex I and then passed to Coenzyme Q (CoQ). $FADH_2$ also contributes electrons to CoQ, by Complex II. Together, these electrons are passed to Complex III and then distributed to cytochrome c and then to Complex IV. The final stage of the ETC occurs when the electrons move from Complex IV to be accepted by O_2 to form water.

As the processes of the ETC progress, many protons start to collect in the intermembrane space of mitochondria. These protons are directly used to generate ATP during cellular respiration through reaction with ATP synthase. Also named complex V, ATP synthase uses free energy of an electrochemical gradient of protons generated by the respiratory chain through oxidative phosphorylation. After its production, ATP will then be moved to where it is needed within the cell through diffusion [2].

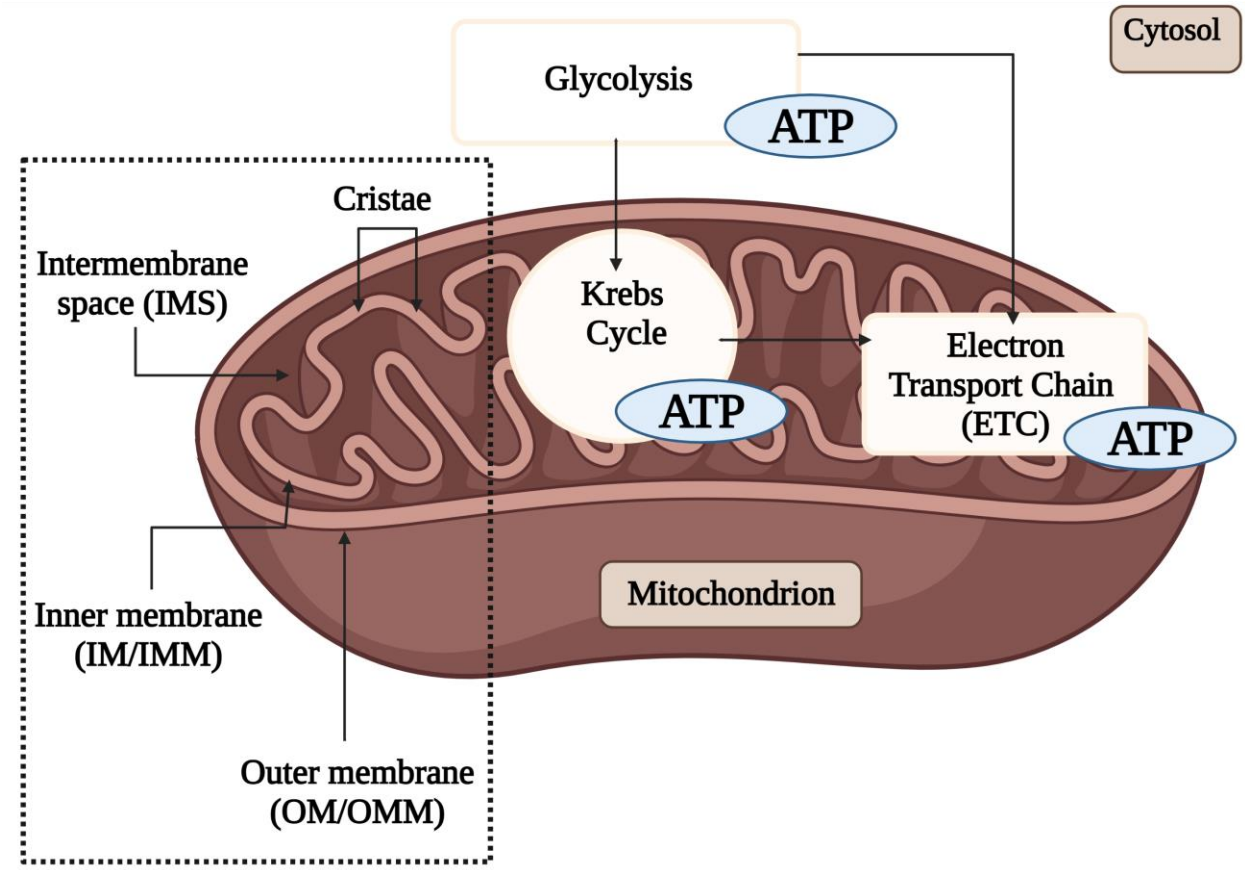

Figure 1.1 Graphical overview of mitochondrial structure and function

Illustrated above are the structures of the mitochondrion previously mentioned: the outer membrane (OMM), inner membrane (IMM) that contain inner folding or cristae, separated by an intermembrane space (IMS) and the matrix compartment. These structures are the site of cellular respiration and energy productions as adenosine triphosphate (ATP).
Created with BioRender.com

Cytosol

The cytosol, also known as the intracellular fluid or cytoplasmic matrix, is the liquid component of the cell in which organelles and proteins suspend. The cytosol serves as the facilitator for many intracellular processes. Cellular processes that have been found to occur in the cytosol include signal transduction, structural support in eukaryotes and supporting functions such as DNA transcription/replication and glycolysis in prokaryotes which lack membrane-bound organelles [1].

Endoplasmic Reticulum

The endoplasmic reticulum is a compartment composed of a network of interconnected membrane-bounded vesicles called cisternae [1] which is found in most eukaryotic cells. The ER most importantly participates in the synthesis of many membrane lipids and proteins. Essentially the ER is the transportation system of the cell in eukaryotes. It has two subunits: the rough endoplasmic reticulum (RER) and smooth endoplasmic reticulum (SER).

The Smooth Endoplasmic Reticulum

The SER usually makes up the least volume of the ER. The synthesis of fatty acids and phospholipids occurs in the smooth ER. The presence of SER allows for an increased surface area to be devoted to the storage of enzymes and their products. In most cell sites the volume of SER is low, there are instead transitional ERs that contain ER exit sites where proteins assembled in the ER transition to the Golgi apparatus [2].

The Rough Endoplasmic Reticulum

The RER is covered with ribosomes, the macromolecular complex that produces protein, giving it a "rough" appearance [2]. Translating ribosomes are bonded to the RER membrane presumably by ribosome receptors [11]. During translation as the growing secretory polypeptide emerges from the ribosome, it passes through the rough ER membrane with the facilitation of membrane proteins [2]. Newly produced secretory proteins then collect in the inner space (lumen) of the rough ER before being transported out of the ER to their next designated location. Since the ER is necessary for synthesis of plasma-membrane proteins and proteins of the extracellular matrix all eukaryotic cells have a conserved content of this organelle for efficient function.

Lysosome

Lysosomes are organelles that are responsible for managing the waste of the cell. Lysosomes are the site of a variety of enzymes that allow the cell to break down macromolecules such as peptides, nucleic acids, carbohydrates, and lipids. In addition, the lysosome is also capable of fusing with other organelles [2] and digesting large structures or cellular debris. Enzymes of the lysosomes are produced in the RER and exported to the Golgi apparatus upon recruitment [12]. Enzymes that are meant to be transported to the lysosome are specifically marked with mannose 6-phosphate, allowing for them to be bonded to mannose-6-phosphate receptors in the Golgi apparatus. The enzymes are then properly placed into acidified vesicles which later fuse with a late endosome. This fusion allows for the dissociation of the lysosomal enzyme and mannose 6-phosphate receptors and further transport into established lysosomes [1].

Organelle-Organelle Interaction

For the cell to work efficiently as a biological system, organelles are required to coordinate their activities. Organelle-organelle membrane contact sites (MCSs) are centers for the transfer of ions, lipids and proteins and organelle remodeling [13]. Functionality of membrane contact sites associated with the endoplasmic reticulum (ER) are the best described. The ER has organelle-organelle contacts with the plasma membrane, endosome, lysosomes, mitochondria, and peroxisomes. In *Saccharomyces cerevisiae* an ER-mitochondria encounter structure (ERMES), a protein complex at the ER-mitochondria MCSs, was identified to have a role in Ca^{2+} signaling [14, 15]. The ERMES complex is also involved in maintaining iron homeostasis [16]. There is increasing interest in the interplay between mitochondria and lysosomes as they are both critical for maintaining cellular homeostasis. Dysfunction in either of these organelles is linked to multiple human diseases [17]. Like other organelle-organelle MCS mitochondria-lysosome sites may similarly mediate the transfer of lipids, calcium, or iron between mitochondria and lysosomes. Of particular importance for precedence in this is the example of iron.

Iron can be stored by both mitochondrial and endolysosomal compartments. Entry of iron into mitochondria is facilitated by mitoferrin-1 and mitoferrin-2 both are mitochondrial carrier family proteins in the IMM. Mitochondrial iron, then incorporated into iron-sulfur clusters and heme in the matrix. [18,19]. Mitochondria–lysosome MCS may be connected to the labile iron pool, a function like mitochondria–endosome contact sites. Interestingly, in fibroblasts from patients with brain iron accumulation causes mitochondrial depolarization, reduced ATP

production, and decreased lysosomal proteolytic activity [20]. This finding draws a connection between mitochondria–lysosome contact site dysfunction and iron flux.

Also, in *S. cerevisiae*, contact sites have been identified between mitochondria and the vacuole. This site known as the vacuole and mitochondria patch (vCLAMP) regulates the movement of phospholipids between mitochondria and vacuoles [21,22]. The vacuole of *S. cerevisiae*, equivalent to the lysosome in mammalian cells, is responsible for bulk degradation of proteins and storing ions of the cell. [23]. Recently, scientists have shown that intracellular iron limitation is due to vacuole-mediated mitochondrial inhibitors. The authors interestingly highlight that cysteine accumulation causes an oxygen-dependent oxidative stress which leads to iron limitation. The findings of this study demonstrate that cysteine-mediated iron deprivation is connected to vacuole-mediated mitochondrial dysfunction forming a comprehensive mechanism that showed vacuole-mediated cysteine compartmentation influences iron bioavailability and mitochondria function [24].

1.2 Copper and iron transport as they relate to human disease

Copper and iron are essential elements for all eukaryotes. Transition metals are important factors of redox reactions because of their ability to easily gain and lose electrons. This ability can also render transition metals potentially toxic. Due to their potentially toxic nature, cells must use several mechanisms to maintain homeostasis and protect against toxicity. Transmembrane transport is one of several mechanisms identified that maintains the balance of metals in the cell that are required for biological processes. Cells contain multiple transport systems with overlapping specificity for substrates although they are genetically separable [25]. Genes attributable to human disease have continually been researched as factors that influence transition-metal metabolism, contributing to advances of understanding transition-metal transport. Also, recent investigations using *Saccharomyces cerevisiae* have given much understanding to metal metabolism within the cell. (Table 1).

Table 1.1 Genes that affected transition metal metabolism in humans and yeast

Phenotype of yeast disruption	Protein	Human homolog	Phenotype of mammalian disruption
Deficient growth on low Fe	Fet3	Ceruloplasmin	Deficient iron mobilization
Deficient growth on low Fe/Cu	Ctr1	hCtr1	Embryonic lethality
Deficient growth on low Fe/Cu	Atx1	Atox1	Pre-weaning lethality
Deficient growth on low Fe/Cu	Ccc2	Menkes (Atp7a)	Severe copper deficiency
		Wilson (Atp7b)	Copper overload
Deficient growth on low Mn	Smf1/Smf2	Nramp2	Microcytic anemia due to deficient iron transport
Deficient growth on non-fermentable carbon sources due to mitochondrial iron overload	Yfh1	Frataxin	Decreased amounts of protein cause Friedreich's ataxia

Table modified from Askwith and Kaplan [1].

Iron Transport

To date there have been at least two proteins named that are directly involved in transmembrane transport of iron in humans [26, 27]. Fet3p is a multicopper oxidase that mediates high-affinity iron transport in *Saccharomyces cerevisiae*. It is a part of a bipartite system that includes both Ftr1p, a transmembrane iron permease, and Fet3p, an integral membrane protein with an extracellular multicopper oxidase domain. Fet3p transports iron by converting ferrous iron to ferric iron, which in turn is transported by Ftr1p [28,29]. Fet3p substrates are produced by ferric reductases that are located on the cell surfaces that are needed to mediate electron transport to reduce ferric iron and cupric copper [30,31]. There have been great advances in understanding transport of iron but further investigation in understanding the exact mechanisms. Interestingly, through the search for identifying iron transporters scientists have also learned more about human copper transporters.

Copper Transport

The transport of copper depends on a series of proteins. Ctr1, originally discovered in yeast, transports copper into the cell [32]. Once in the cell Cu^{+} goes to copper chaperones Atox1, Cox17 or CCS. Atox1 interacts with Atp7b in the hepatocyte and ATP7A in other cell types. This interaction between Atox1 and Atp7b makes it important for proper biliary excretion of copper which is the sole export pathway for copper from the body. Atox1 is also essential to the delivery of copper to the secretory pathways in the trans Golgi network [33]. Cox17, another copper chaperone, delivers copper to assembly proteins within the mitochondrial IMS [34]. CCS,

the second copper chaperone to be identified, is required to deliver copper to SOD which is needed for detoxification of ROS [35].

Copper chaperones are proteins that deliver copper to specific copper-containing enzymes such as SOD and COX. Cuproenzymes in the secretory pathway depend on ATP7A and ATP7B for their transport. Newly absorbed dietary copper enters the liver and leaves as ceruloplasmin or is excreted in bile. In the case of WD, ATP7B is mutated leading to decreased serum ceruloplasmic levels and increased copper concentrations in the liver. ATP7A is not expressed in hepatocytes but is important for copper delivery to neurons and astrocytes [36]. Dysfunction of the regulation of transition metals has a strong connection to human health and diseases. Identification of novel pathways that are associated with uptake, storage and detoxification can lead to optimizing diagnosis and treatment of transition-metal related diseases.

1.3 Wilson Disease

Wilson Disease (WD) is a rare, inherited disease of copper metabolism. While it was first described by Kinnier Wilson in the early 1900s, copper's involvement in the pathogenesis of WD was not established until the 1990s [37, 38, 39]. WD is the result of a mutation of the ATP7B gene and is inherited as an autosomal recessive trait. The ATP7B protein is involved in delivering copper into ceruloplasmin, a copper-carrying protein in the blood, and in biliary copper excretion. Wilson disease protein ATP7B utilizes lysosomal exocytosis to maintain copper homeostasis [40]. Mutation of ATP7B results in less than satisfactory synthesis of ceruloplasmin, defective biliary copper excretion and ultimately copper accumulation in hepatic and extrahepatic tissues. This accumulation leads to copper toxicity and many negative clinical manifestations in several organs, but most importantly the liver and brain [41]. A key consequence of copper accumulation in WD includes liver disease and subsequent neurological disorders. This liver damage induced by excess copper can range from acute hepatitis to acute liver failure and cirrhosis [42]. Treatment for WD aims to rebalance copper levels with drugs that chelate the copper, reduce absorption or both. However, in patients that do not respond well to medical treatment, a liver transplantation is needed. Without treatment and management WD is fatal. Treatment, such as chelation therapy, is palliative and must be followed strictly to prevent copper accumulation from occurring again [43].

The assembly of the cytochrome c oxidase in the electron transport chain and therefore respiration, is highly dependent on copper recruitment to mitochondria. To maintain supply and avoid toxicity, copper uptake, storage and release are tightly controlled. These molecular mechanisms are especially important in diseases of copper overload such as

WD. In WD patients and animal models, mitochondria are directly damaged by copper overload. This leads to mitochondrial structural alterations and bioenergetic impairments. Copper-mediated damage to mitochondria seen in WD patient hepatocytes directly correlates to severe clinical symptoms such as liver failure and death [44].

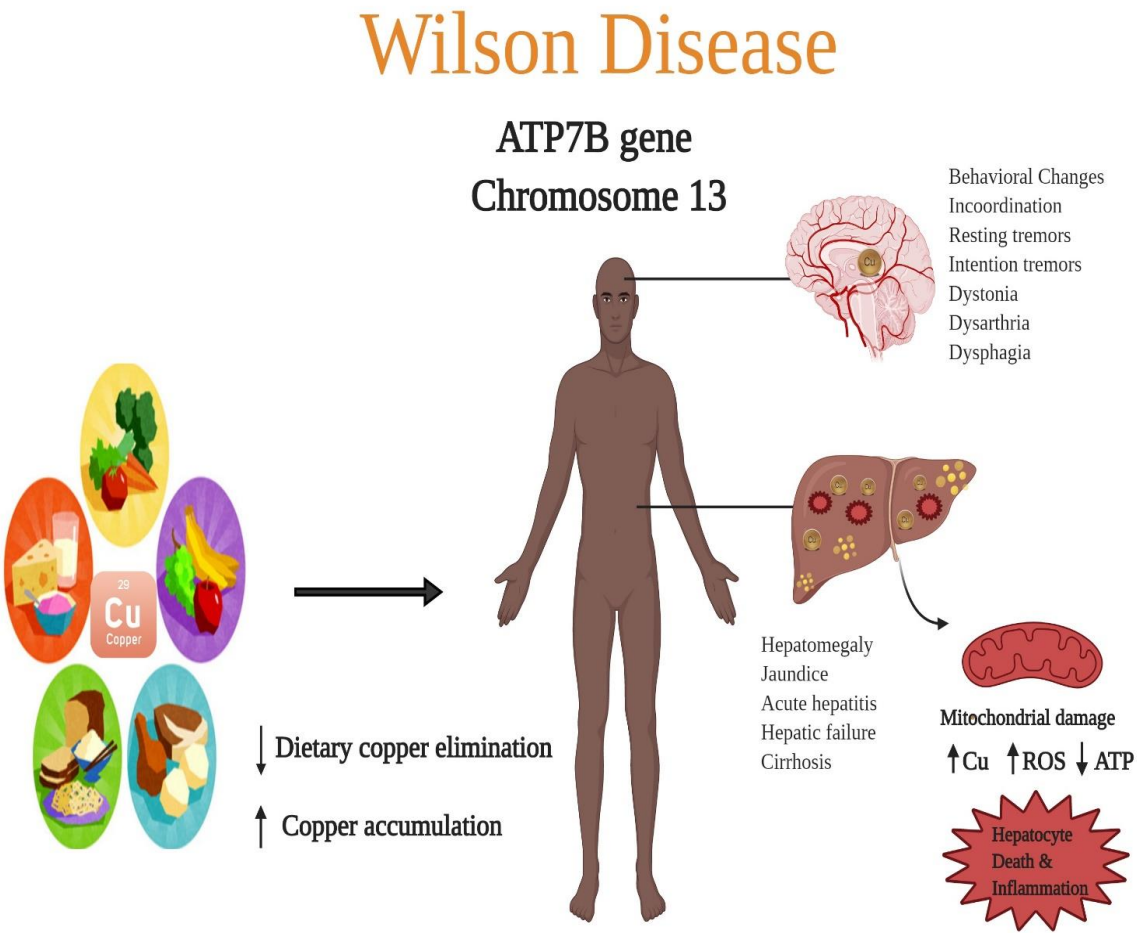

Figure 1.2 Graphical pathogenesis of Wilson Disease

Illustrated here is the pathogenesis of Wilson Disease (WD). In WD, toxic copper accumulation occurs due to improper copper excretion from the body. Excess copper directly impairs mitochondria causing structural alterations and dysfunction in important processes such as cellular respiration. Created with Biorender.com.

1.4 Consequences of oxidative stress

Copper accumulation in hepatic cells leads to defects in bioenergetic processes and to alterations in mitochondrial structure. The exact, hepatic response to these energetic defects is not completely understood. It is hypothesized that copper accumulation in WD leads to an imbalance of ROS and overproduction of free radicals can lead to damage to proteins, lipids, and DNA [45]. A target of the ROS induced damage is the mitochondrial respiratory chain, located in the IMM [46, 47]. Damage to the complexes of the ETC and the lipids of the IMM can have major consequences for ATP production.

Normally, the IM is selectively permeable to neutral small molecules. However, the IMM, near the site of ROS production, is prone to lipid peroxidation [48, 49]. When mitochondrial phospholipids experience peroxidation it leads to increased proton permeability of the IMM [50], leading to modulations of biophysical properties of mitochondrial membranes and impaired biochemical functions of various transporters and respiratory enzymes in the inner and outer membranes. Also, respiratory enzymes like succinate dehydrogenase and nicotinamide adenine dinucleotide dehydrogenase contain iron sulfur centers which are susceptible to oxidative modification impairing the electron-transport function of mitochondria [51].

Thiols are organic compounds that contain a sulfhydryl (S-H) group. Thiols are the most abundant available antioxidants in the body and play an important role in defense against ROS. In the cell thiols occur in the free form as oxidized or reduced glutathione (GSH). Decreased levels of thiols have been noted in a range of diseases including chronic renal failure, cardiovascular disorders, stroke and neurological disorders and alcoholic cirrhosis [52]. Additionally, mitochondrial protein thiols have also been identified as a target

for unbound copper ions during copper accumulation in the Long-Evans Cinnamon (LEC) rat which is an animal model for WD that shows similar clinical and biochemical features. In this model copper overload oxidation of the protein thiols in the mitochondria causes membrane crosslinking and ultimately structural alterations on the membranes and cristae [53].

1.5 Heme and Fe-S Clusters Biosynthesis

Heme and Fe-S clusters are important cofactors in the cell. Most of the total iron content is used in heme containing proteins such as cytochromes, catalases, peroxidases, and hemoglobin. Heme is used in many biological processes, including photosynthesis, oxygen transport, oxidation, and reduction, and many more. [54]. Heme's biological importance has meant that nearly every organism has the conserved biosynthetic pathway to synthesize heme. In eukaryotes heme biosynthesis starts with the synthesis of δ-aminolaevulinic acid (dALA or δALA) from the amino acid glycine and succinyl-CoA from the Krebs cycle [55]. ALA synthase is required for the reaction and is regulated by heme concentration. ALA is then exported from the mitochondrion to the cytosol, two molecules of ALA go through condensation to form porphobilinogen (PBG) by the enzyme porphobilinogen synthase (PBGS) or ALA dehydratase (ALAD) [56, 57]. PBG molecules are converted to linear tetrapyrrole by porphobilinogen deaminase (PBGD) [58]. This molecule serves as the precursor for uroporphyrinogen synthase (UROS) which forms uroporphyrinogen III. Coprophyrinogen III is then formed from uroporphyrinogen III which is eventually decarboxylated by uroporphyrinogen decarboxylase (UROD) in the cytosol [59]. In the final steps of heme biosynthesis coprophyrinogen enters mitochondria and undergoes oxidative decarboxylation to form protoporphyrinogen IX by coproporphyrinogen III oxidase (CPO) [60, 61]. Protoporphyrinogen IX is then oxidized by protoporphyrinogen IX oxidase (PPO) to form protoporphyrin IX (PPIX) [62].

Ferrochelatase (FC) then inserts ferrous iron into PPIX to form Fe-protoporphyrin IX or heme [63]. Once this process is complete, heme can undergo modifications to their side chain (ex: heme A and heme O synthesis) or covalent attachments (ex: heme C in cytochrome c biogenesis) to produce additional heme types depending on cellular needs.

Fe-S cluster Biogenesis: general pathway

Fe-S cluster biogenesis is highly conserved in all kingdoms of life. It is an extremely intricate machinery for Fe-S cluster biogenesis in eukaryotes and for mitochondria that encompasses up to 18 proteins. Many of the general steps of this pathway are common among varying organisms.

There has not been a proven specified source of iron for the Fe-S cluster synthesis, while initial studies suggested iron may be donated from acidic patches on frataxin, an iron binding protein, this was later refuted as the only specific role for frataxin appears to be in handling of sulfur for the clusters [64, 65]. The initial stages of Fe-S cluster biogenesis are carried out by a protein complex of cysteine desulfurase (NFS1) bound to iron-sulfur cluster assembly enzyme (ISCU) and iron-sulfur cluster scaffold protein (NFU1) (Figure 1.2) [67, 68, 69]. The stability of cysteine desulfurase depends on its binding to ISD11, a protein found in the mitochondrial matrix of *S. cerevisiae* and mammalian cells [66]. The protein frataxin (Yfh1 in *S. cerevisiae*) then binds in between NFS1 and ISCU (Figure 1.2) where it participates in a conformational change to enhance cluster formations [70]. The emerging clusters rely on a source of electron donors identified in previous findings to include: glutaredoxin 5 (GLRX5) [71], ferredoxin [72] and possibly glutathione [73]. After an Fe-S cluster is successfully formed, it is transferred to recipient proteins [74].

Fe-S clusters are susceptible to oxidative damage and disruption of its biogenesis causes a myriad of human diseases. Emergence of harmful ROS and oxidative damage is a hallmark of copper accumulation and WD. To date cellular damage in disease characterized by copper accumulation, like WD, has not been connected to iron dependent processes like Fe-S cluster biogenesis and heme biosynthesis.

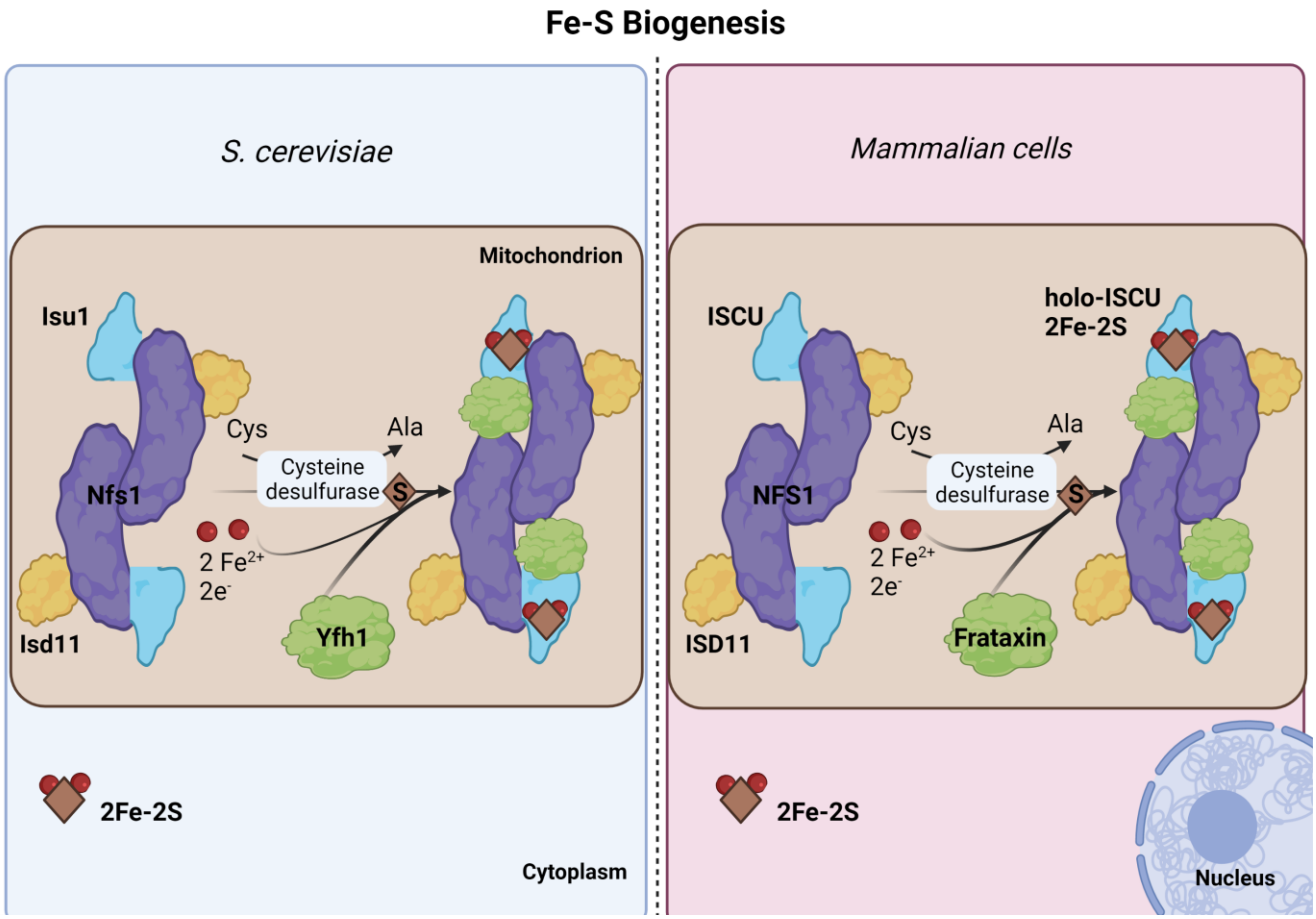

Figure 1.3 A general scheme for biogenesis of Fe-S clusters in *Saccharomyces cerevisiae* and mammalian cells

An outline of the basic steps of iron sulfur (Fe-S) cluster biogenesis only. NFS1 (Nfs1) is a cysteine desulfurase bound to primary scaffold protein ISCU (Isu1) and ISD11 (Isd11). Frataxin (Yfh1) forms part of the Fe-S cluster biogenesis complex by possibly binding to a space between NFS1 (Nfs1) and ISCU (Isu1). ISCU (Isu1) houses the synthesis of Fe-S clusters, where Yfh1/frataxin donates iron and NFS1/Nfs1 serves as a donor of inorganic sulfur.

1.6 The connectivity of iron and copper transport systems

The mitochondrial carrier family (MCF) is a family of proteins involved in translocation of TCA intermediates, nucleoside di- and triphosphates, and other substrates across the mitochondrial inner membrane (IM) [75]. Some MCF proteins are known to play a role in balancing metal concentrations in mitochondria. Iron transport in the mitochondria has been linked to three MCF proteins: *MRS3, MRS4* and *RIM2*. Mitochondrial carrier proteins *MRS3* and *MRS4* were identified as high-affinity iron transporters across the IM [76,77] while Rim2 was also shown to mediate transport of nucleotide-bound iron across the IM in yeast [78]. Other MCF proteins who have some contribution to mitochondrial iron concentration balance include mitochondrial carrier protein (Mtm1) and glutathione-specific gamma-glutamylcyclotransferase (Ggc1) [78]. Mtm1 and Ggc1 also importantly demonstrated that MCFs can indirectly modify metal-related phenotypes in yeast.

For copper MCF family member Pic2 has been shown to act as a copper importer in yeast. In many organisms Pic2 homologs act as mitochondrial phosphate carriers, but in *Saccharomyces cerevisiae* Mir1 is the primary phosphate carrier [80]. In findings from Vest et al. (2016) mitochondria from *pic2Δ* mutants still had the ability to uptake copper though it was at lower measured concentrations when compared to wild type. This and previous results provided clarification that Pic2 is not the sole protein responsible for mitochondrial copper import [76, 79]. It was shown in this study and others using various homologs of Mrs3 that this protein is capable of copper transport. In a computational analysis Pic2 was shown to share a similarity with Mrs3 in two regions predicted to mediate substrate binding, including a histidine residue that was recently shown to be involved in iron transport [81, 82]. This redundancy allows

some margin for flexibility in substrate binding, in these proteins allowing iron carriers to be involved in mitochondrial copper import.

Iron metabolism in Wilson Disease

Copper and iron metabolism overlap in many different metabolic pathways [74,79]. This leads to clinical symptoms in patients with WD that are attributed to compromised copper and iron metabolism. In an experimental WD model accumulation of copper and iron in the liver were noted [83,84]. In addition to these findings, other studies have suggested that iron metabolism is impaired in WD and iron accumulation in the liver and/or brain tissue may worsen the clinical progression and symptoms of the disease [85,86]. Other significant findings indicate that changes in copper metabolism are parallel to changes in iron metabolism in WD. Chelating therapies restore but do not normalize iron metabolism [87]. Exploring copper-iron interactions broadens the potential to improve patient treatment and better understand underlying mechanisms of WD. Because of this, expanding in understanding of the connections between the two should prove to be an important area of investigation.

Overall aim of this thesis

The overlap of copper and iron systems prove an interesting area of research as it relates to molecular processes and human disease. In this thesis I provide evidence that copper accumulation leads to changes in the thiol containing molecules within mitochondria and disruption of the heme biosynthesis pathway. Further development of understanding and treatment requires molecular characterization of specific protein. Results of this study and further investigation will increase our understanding of mitochondrial copper import and the mechanisms involved in mitochondrial copper.

References

1. Lodish, H., Berk, A., Zipursky, S.L., et al. (2000) Molecular Cell Biology. (4th ed.) *New York: W. H. Freeman* Section 5.4, Organelles of the Eukaryotic Cell.
2. Alberts, B., Johnson, A., Lewis, J., Raff, M., Roberts, K., Walter P. (2002). Molecular biology of the cell (4th ed.). *New York: Garland Science*.
3. Cooper, G. M. (2000) The Cell: A Molecular Approach. (2nd ed.) *Sinauer Associates.*
4. Almén, M. S., Nordström, K. J., Fredriksson, R., Schiöth, H. B. (2009) Mapping the human membrane proteome: a majority of the human membrane proteins can be classified according to function and evolutionary origin. *BMC biology*, *7*, 50
5. Lin, Y., Fuerst, O., Granell, M., Leblanc, G., Lórenz-Fonfría, V., Padrós, E. (2013). The substitution of Arg149 with Cys fixes the melibiose transporter in an inward-open conformation. *Biochimica et biophysica acta*, 1828, 1690–1699.
6. Cappellaro, C., Baldermann, C., Rachel, R., Tanner, W. (1994) Mating type-specific cell-cell recognition of *Saccharomyces cerevisiae*: cell wall attachment and active sites of a- and alpha-agglutinin. *EMBO J*.13, 4737–4744.
7. Baba, M., Osumi, M., (1987) Transmission and scanning electron microscopic examination of intracellular organelles in freeze-substituted Kloeckera and Saccharomyces cerevisiae yeast cells. *J. Electron Microsc.* Tech.5, 249–261.
8. de Nobel, J. G., Klis, F. M., Priem, J., Munnik, T., van den Ende, H. (1990). The glucanase-soluble mannoproteins limit cell wall porosity in Saccharomyces cerevisiae. *Yeast (Chichester, England)* 6, 491–499.
9. Fry, S. C. (1986) Cross-linking of matrix polymers in the growing cell walls of angiosperms. *Ann. Rev. Plant. Physiol*., 37, 165-186.
10. Lipke, P. N., Ovalle, R. (1998) Cell wall architecture in yeast: new structure and new challenges. *Journal of bacteriology*, 180, 3735–3740.
11. Klis, F. M., Mol, P., Hellingwerf, K., Brul, S. (2002) Dynamics of cell wall structure in Saccharomyces cerevisiae. *FEMS microbiology reviews*, 26, 239–256.
12. Bajaj, L., Sharma, J., di Ronza, A., Zhang, P., Eblimit, A., Pal, R., Roman, D., Collette, J. R., Booth, C., Chang, K. T., Sifers, R. N., Jung, S. Y., Weimer, J. M., Chen, R., Schekman, R. W., Sardiello, M. (2020) A CLN6-CLN8 complex recruits lysosomal enzymes at the ER for Golgi transfer. *The Journal of clinical investigation,* 130, 4118–4132.
13. Helle, S. C., Kanfer, G., Kolar, K., Lang, A., Michel, A. H., Kornmann, B. (2013) Organization and function of membrane contact sites. *Biochimica et biophysica acta*, 1833, 2526–2541.
14. Phillips, M. J., Voeltz, G. K. (2016) Structure and function of ER membrane contact sites with other organelles. *Nature reviews. Molecular cell biology*, 17, 69–82.
15. Kornmann, B., Currie, E., Collins, S. R., Schuldiner, M., Nunnari, J., Weissman, J. S., Walter, P. (2009) An ER-mitochondria tethering complex revealed by a synthetic biology screen. *Science, (New York, N.Y.)* 325, 477–48.
16. Wong, Y. C., Kim, S., Peng, W., Krainc, D. (2019) Regulation and Function of Mitochondria-Lysosome Membrane Contact Sites in Cellular Homeostasis. *Trends in cell biology*, 29, 500–513.
17. Richardson, D. R., Lane, D. J., Becker, E. M., Huang, M. L., Whitnall, M., Suryo Rahmanto, Y., Sheftel, A. D., Ponka, P. (2010) Mitochondrial iron trafficking and the

integration of iron metabolism between the mitochondrion and cytosol. *Proceedings of the National Academy of Sciences of the United States of America*, 107, 10775–10782.
18. Rouault T. A. (2012) Biogenesis of iron-sulfur clusters in mammalian cells: new insights and relevance to human disease. *Disease models & mechanisms*, 5, 155–164.
19. Seibler, P., Burbulla, L. F., Dulovic, M., Zittel, S., Heine, J., Schmidt, T., Rudolph, F., Westenberger, A., Rakovic, A., Münchau, A., Krainc, D., Klein, C. (2018) Iron overload is accompanied by mitochondrial and lysosomal dysfunction in WDR45 mutant cells. *Brain: a journal of neurology*, 14, 3052–3064.
20. Elbaz-Alon, Y., Rosenfeld-Gur, E., Shinder, V., Futerman, A. H., Geiger, T., Schuldiner, M. (2014) A dynamic interface between vacuoles and mitochondria in yeast. *Developmental cell*, 30, 95–102.
21. Hönscher, C., Mari, M., Auffarth, K., Bohnert, M., Griffith, J., Geerts, W., van der Laan, M., Cabrera, M., Reggiori, F., Ungermann, C. (2014) Cellular metabolism regulates contact sites between vacuoles and mitochondria. *Developmental cell*, 30, 86–94.
22. Thumm, M. (2000) Structure and function of the yeast vacuole and its role in autophagy. *Microscopy research and technique*, 51, 563–572.
23. Hughes, C. E., Coody, T. K., Jeong, M. Y., Berg, J. A., Winge, D. R., Hughes, A. L. (2020) Cysteine Toxicity Drives Age-Related Mitochondrial Decline by Altering Iron Homeostasis. *Cell*, 180, 296–310.e18.
24. Askwith, C., Kaplan, J. (1998) Iron and copper transport in yeast and its relevance to human disease. *Trends in biochemical sciences*, 23, 135–138.
25. Andrews N. C. (1999) The iron transporter DMT1. *The international journal of biochemistry & cell biology*, 31, 991–994.
26. Li, S., Yang, Y., & Li, W. (2020) Human ferroportin mediates proton-coupled active transport of iron. *Blood advances*, 4, 4758–4768.
27. Stearman, R., Yuan, D. S., Yamaguchi-Iwai, Y., Klausner, R. D., & Dancis, A. (1996) A permease-oxidase complex involved in high-affinity iron uptake in yeast. *Science (New York, N.Y.)*, 271, 1552–1557.
28. Askwith, C., Eide, D., Van Ho, A., Bernard, P. S., Li, L., Davis-Kaplan, S., Sipe, D. M., Kaplan, J. (1994) The FET3 gene of S. cerevisiae encodes a multicopper oxidase required for ferrous iron uptake. *Cell*, 76, 403–410.
29. Lesuisse, E., Crichton, R. R., Labbe, P. (1990) Iron-reductases in the yeast Saccharomyces cerevisiae. *Biochimica et biophysica acta*, 1038, 253–259.
30. Scheiber, B., Goldenberg, H. (1993) NAD(P)H:ferric iron reductase in endosomal membranes from rat liver. *Archives of biochemistry and biophysics*, 305, 225–230.
31. Peña, M. M., Lee, J., Thiele, D. J. (1999) A delicate balance: homeostatic control of copper uptake and distribution. *The Journal of nutrition*, 129, 1251–1260.
32. Prohaska, J. R., Gybina, A. A. (2004) Intracellular copper transport in mammals. *The Journal of nutrition*, 134, 1003–1006.
33. Carr, H. S., Winge, D. R. (2003) Assembly of cytochrome c oxidase within the mitochondrion. *Accounts of chemical research*, 36, 309–316
34. Culotta, V. C., Klomp, L. W., Strain, J., Casareno, R. L., Krems, B., Gitlin, J. D. (1997) *The copper chaperone for superoxide dismutase. The Journal of biological chemistry*, 272, 23469–23472.
35. Wilson, S. A. K. (1912) The Wilson disease gene is a putative copper transporting P-type ATPase similar to the Menkes gene. *Brain* 34, 295-507.

36. Bull, P. C., Thomas, G. R., Rommens, J. M., Forbes, J. R., Cox, D. W. (1993) The Wilson disease gene is a putative copper transporting P-type ATPase similar to the Menkes gene. *Nature genetics*, 5, 327–337.
37. Tanzi, R. E., Petrukhin, K., Chernov, I., Pellequer, J. L., Wasco, W., Ross, B., Romano, D. M., Parano, E., Pavone, L., Brzustowicz, L. M. (1993) The Wilson disease gene is a copper transporting ATPase with homology to the Menkes disease gene. *Nature genetics*, 5, 344–350.
38. Patil, M., Sheth, K. A., Krishnamurthy, A. C., Devarbhavi, H. (2013) A review and current perspective on Wilson disease. *Journal of clinical and experimental hepatology*, 3, 321–336.
39. Polishchuk, E. V., Concilli, M., Iacobacci, S., Chesi, G., Pastore, N., Piccolo, P., Paladino, S., Baldantoni, D., van IJzendoorn, S. C., Chan, J., Chang, C. J., Amoresano, A., Pane, F., Pucci, P., Tarallo, A., Parenti, G., Brunetti-Pierri, N., Settembre, C., Ballabio, A., Polishchuk, R. S. (2014) Wilson disease protein ATP7B utilizes lysosomal exocytosis to maintain copper homeostasis. *Developmental cell*, 29, 686–700.
40. Roberts, E. A., Schilsky, M. L., American Association for Study of Liver Diseases (AASLD) (2008) Diagnosis and treatment of Wilson disease: an update. *Hepatology (Baltimore, Md.)*, 47, 2089–2111.
41. Zischka, H., Borchard S. (2018) Chapter 8 - Mitochondrial Copper Toxicity with a Focus on Wilson Disease.Clinical and Translational Perspectives on WILSON DISEASE. *Academic Press*, 65-75.
42. Mazi, T. A., Shibata, N. M., Medici, V. (2020) Lipid and energy metabolism in Wilson disease. *Liver research*, 4, 5–14.
43. Douarre, C., Sourbier, C., Dalla Rosa, I., Brata Das, B., Redon, C. E., Zhang, H., Neckers, L., & Pommier, Y. (2012) Mitochondrial topoisomerase I is critical for mitochondrial integrity and cellular energy metabolism. *PloS one*, 7, e41094.
44. Chen, J. Q., Yager, J. D., Russo, J. (2005) Regulation of mitochondrial respiratory chain structure and function by estrogens/estrogen receptors and potential physiological/pathophysiological implications. *Biochimica et biophysica acta*, 1746, 1–17.
45. Vajrala, V., Claycomb, J. R., Sanabria, H., Miller, J. H., Jr (2008) Effects of oscillatory electric fields on internal membranes: an analytical model. *Biophysical journal*, 94 2043–2052.
46. Kirkinezos, I. G., Bacman, S. R., Hernandez, D., Oca-Cossio, J., Arias, L. J., Perez-Pinzon, M. A., Bradley, W. G., Moraes, C. T. (2005) Cytochrome c association with the inner mitochondrial membrane is impaired in the CNS of G93A-SOD1 mice. *The Journal of neuroscience: the official journal of the Society for Neuroscience*, 25, 164–172.
47. Stewart, V. C., Heales, S. J. (2003) Nitric oxide-induced mitochondrial dysfunction implications for neurodegeneration. *Free Radic Biol Med*, 34, 287-303.
48. Wei, Y. H., Lu, C. Y., Wei, C. Y., Ma, Y. S., Lee, H. C. (2001) Oxidative stress in human aging and mitochondrial disease-consequences of defective mitochondrial respiration and impaired antioxidant enzyme system. *The Chinese journal of physiology*, 44, 1–11.
49. Mungli, P., Shetty, M. S., Tilak, P.., Anwar, N. (2009) Total Thiols: Biomedical Importance And Their Alteration In Various Disorders. [Journal (On-line/Unpaginated)]
50. Borchard, S., Bork, F., Rieder, T., Eberhagen, C., Popper, B., Lichtmannegger, J., Schmitt, S., Adamski, J., Klingenspor, M., Weiss, K. H.,Zischka, H. (2018) The exceptional

sensitivity of brain mitochondria to copper. *Toxicology in vitro : an international journal published in association with BIBRA*, 51, 11–22.
51. Tsiftsoglou, A. S., Tsamadou, A. I.., Papadopoulou, L. C. (2006) Heme as key regulator of major mammalian cellular functions: molecular, cellular, and pharmacological aspects. *Pharmacology & therapeutics*, 111, 327–345.
52. Shemin, D., & Rittenberg, D. (1946) The biological utilization of glycine for the synthesis of the protoporphyrin of hemoglobin. *The Journal of biological chemistry*, 166, 621–625.
53. Falk, J. E., Dresel, E. I., Rimington, C. (1953) Porphobilinogen as a porphyrin precursor, and interconversion of porphyrins, in a tissue system. *Nature*, 172, 292–294.
54. Gibson, K. D., Neuberger, A., & Scott, J. J. (1955) The purification and properties of delta-aminolaevulic acid dehydrase. *The Biochemical journal*, 61, 618–629.
55. Shoolingin-Jordan, P. M., Al-Dbass, A., McNeill, L. A., Sarwar, M., Butler, D. (2003) Human porphobilinogen deaminase mutations in the investigation of the mechanism of dipyrromethane cofactor assembly and tetrapyrrole formation. *Biochemical Society transactions*, 31, 731–735.
56. Whitby, F. G., Phillips, J. D., Kushner, J. P., Hill, C. P. (1998) Crystal structure of human uroporphyrinogen decarboxylase. *The EMBO journal*, 17, 2463–2471.
57. Taketani, S., Yoshinaga, T., Furukawa, T., Kohno, H., Tokunaga, R., Nishimura, K., Inokuchi, H. (1995) Induction of terminal enzymes for heme biosynthesis during differentiation of mouse erythroleukemia cells. *European journal of biochemistry*, 230, 760–765.
58. Phillips, J. D., Whitby, F. G., Warby, C. A., Labbe, P., Yang, C., Pflugrath, J. W., Ferrara, J. D., Robinson, H., Kushner, J. P., Hill, C. P. (2004) Crystal structure of the oxygen-dependant coproporphyrinogen oxidase (Hem13p) of Saccharomyces cerevisiae. *The Journal of biological chemistry*, 279, 38960–38968.
59. Porra, R. J., Falk, J. E. (1964) The enzymic conversion of coproporphyrinogen 3 into protoporphyrin 9. *The Biochemical journal*, 90, 69–75.
60. Burden, A. E., Wu, C., Dailey, T. A., Busch, J. L., Dhawan, I. K., Rose, J. P., Wang, B., Dailey, H. A. (1999) Human ferrochelatase: crystallization, characterization of the [2Fe-2S] cluster and determination that the enzyme is a homodimer. *Biochimica et biophysica acta*, 1435, 191–197.
61. Stemmler, T. L., Lesuisse, E., Pain, D., Dancis, A. (2010) Frataxin and mitochondrial FeS cluster biogenesis. *The Journal of biological chemistry*, 285, 26737–26743.
62. Qi, W., Cowan, J. A. (2011) Mechanism of glutaredoxin-ISU [2Fe-2S] cluster exchange. *Chemical communications (Cambridge, England)*, 47, 4989–4991.
63. Shi, Y., Ghosh, M. C., Tong, W. H., Rouault, T. A. (2009) Human ISD11 is essential for both iron-sulfur cluster assembly and maintenance of normal cellular iron homeostasis. *Human molecular genetics*, 18, 3014–3025.
64. Land, T., Rouault, T. A. (1998) Targeting of a human iron-sulfur cluster assembly enzyme, nifs, to different subcellular compartments is regulated through alternative AUG utilization. *Molecular cell*, 2, 807–815.
65. Tong, W. H., Rouault, T. (2000) Distinct iron-sulfur cluster assembly complexes exist in the cytosol and mitochondria of human cells. *The EMBO journal*, 19, 5692–5700.
66. Tong, W. H., Rouault, T. A. (2006) Functions of mitochondrial ISCU and cytosolic ISCU in mammalian iron-sulfur cluster biogenesis and iron homeostasis. *Cell metabolism*, 3, 199–210.

67. Bridwell-Rabb, J., Winn, A. M., Barondeau, D. P. (2011) Structure-function analysis of Friedreich's ataxia mutants reveals determinants of frataxin binding and activation of the Fe-S assembly complex. *Biochemistry*, 50, 7265–7274.
68. Li, K., Besse, E. K., Ha, D., Kovtunovych, G., Rouault, T. A. (2008) Iron-dependent regulation of frataxin expression: implications for treatment of Friedreich ataxia. *Human molecular genetics*, 17, 2265–2273.
69. Shi, Y., Ghosh, M., Kovtunovych, G., Crooks, D. R., Rouault, T. A. (2012) Both human ferredoxins 1 and 2 and ferredoxin reductase are important for iron-sulfur cluster biogenesis. *Biochimica et biophysica acta*, 1823, 484–492.
70. Hider, R. C., Kong, X. L. (2011) Glutathione: a key component of the cytoplasmic labile iron pool. *Biometals : an international journal on the role of metal ions in biology, biochemistry, and medicine*, 24, 1179–1187.
71. Craig, E. A., Marszalek, J. (2002) A specialized mitochondrial molecular chaperone system: a role in formation of Fe/S centers. *Cellular and molecular life sciences : CMLS*, 59, 1658–1665.
72. Palmieri, L., Runswick, M. J., Fiermonte, G., Walker, J. E., Palmieri, F. (2000) Yeast mitochondrial carriers: bacterial expression, biochemical identification and metabolic significance. *Journal of bioenergetics and biomembranes*, 32, 67–77.
73. Vest, K. E., Wang, J., Gammon, M. G., Maynard, M. K., White, O. L., Cobine, J. A., Mahone, W. K., Cobine, P. A. (2016) Overlap of copper and iron uptake systems in mitochondria in Saccharomyces cerevisiae. *Open biology*, 6, 150223.
74. Froschauer, E. M., Schweyen, R. J., Wiesenberger, G. (2009) The yeast mitochondrial carrier proteins Mrs3p/Mrs4p mediate iron transport across the inner mitochondrial membrane. *Biochimica et biophysica acta*, 1788, 1044–1050.
75. Froschauer, E. M., Rietzschel, N., Hassler, M. R., Binder, M., Schweyen, R. J., Lill, R., Mühlenhoff, U., & Wiesenberger, G. (2013) The mitochondrial carrier Rim2 co-imports pyrimidine nucleotides and iron. *The Biochemical journal*, *455*(1), 57–65.
76. Vozza, A., Blanco, E., Palmieri, L., Palmieri, F. (2004) Identification of the mitochondrial GTP/GDP transporter in Saccharomyces cerevisiae. *The Journal of biological chemistry*, 279, 20850–20857.
77. Luk, E., Carroll, M., Baker, M., Culotta, V. C. (2003) Manganese activation of superoxide dismutase 2 in Saccharomyces cerevisiae requires MTM1, a member of the mitochondrial carrier family. *Proceedings of the National Academy of Sciences of the United States of America*, 100, 10353–10357.
78. Vest, K. E., Leary, S. C., Winge, D. R., Cobine, P. A. (2013) Copper import into the mitochondrial matrix in Saccharomyces cerevisiae is mediated by Pic2, a mitochondrial carrier family protein. *The Journal of biological chemistry*, 288, 23884–23892.
79. Hamel, P., Saint-Georges, Y., de Pinto, B., Lachacinski, N., Altamura, N., Dujardin, G. (2004) Redundancy in the function of mitochondrial phosphate transport in Saccharomyces cerevisiae and Arabidopsis thaliana. *Molecular microbiology*, 51, 307–317.
80. Robinson, A. J., Overy, C., Kunji, E. R. (2008) The mechanism of transport by mitochondrial carriers based on analysis of symmetry. *Proc. Natl. Acad. Sci USA*, 105, 17766- 17771.
81. Brallolotto, X., Pierrel, F., Pelosi, L., (2014) Three conserved histidine residues contribute to mitochondrial iron transport through mitoferrins. *Biochem J*, 460, 79-89.

82. Chandarana, H., Lim, R. P., Jensen, J. H., Hajdu, C. H., Losada, M., Babb, J. S., Huffman, S., Taouli, B. (2009) Hepatic iron deposition in patients with liver disease: preliminary experience with breath-hold multiecho T2*-weighted sequence. *AJR. American journal of roentgenology*, 193, 1261–1267.
83. Koizumi, M., Fujii, J., Suzuki, K., Inoue, T., Inoue, T., Gutteridge, J. M., Taniguchi, N. (1998) A marked increase in free copper levels in the plasma and liver of LEC rats: an animal model for Wilson disease and liver cancer. *Free radical research*, 28, 441–450.
84. Litwin, T., Gromadzka, G., Szpak, G. M., Jabłonka-Salach, K., Bulska, E., Członkowska, A. (2013) Brain metal accumulation in Wilson's disease. *Journal of the neurological sciences*, 329, 55–58.
85. Dusek, P., Bahn, E., Litwin, T., Jabłonka-Salach, K., Łuciuk, A., Huelnhagen, T., Madai, V. I., Dieringer, M. A., Bulska, E., Knauth, M., Niendorf, T., Sobesky, J., Paul, F., Schneider, S. A., Czlonkowska, A., Brück, W., Wegner, C., Wuerfel, J. (2017) Brain iron accumulation in Wilson disease: a post mortem 7 Tesla MRI - histopathological study. *Neuropathology and applied neurobiology*, 43, 514–532.
86. Gromadzka, G., Wierzbicka, D., Litwin, T., Przybyłkowski, A. (2021) Iron metabolism is disturbed and anti-copper treatment improves but does not normalize iron metabolism in Wilson's disease. *Biometals : an international journal on the role of metal ions in biology, biochemistry, and medicine*, 34, 407–414.

Chapter 2
Copper induced toxicity in mitochondria

Abstract

A key clinical manifestation of Wilson disease (WD) is copper accumulation in the liver. This leads to a remarkable transformation of diseased hepatocytes in WD, including significant modifications in the mitochondria of hepatocytes. WD has a secondary mitochondrial dysfunction (SMD) caused by copper accumulation because of defects in the *ATP7B* gene. In terms of mitochondrial diseases and modified mitochondrial metabolism, redox modification of mitochondrial proteins is thought to play a key role in regulating cellular responses to oxidative stress. Many mitochondrial proteins contain exposed thiols that are sensitive to oxidation, particularly proteins that are involved in protein import. Modifications to protein thiols likely increase the cell and mitochondria susceptibility to stressors such as proteostasis or increase in mitochondrial based signaling to cell death. While brain mitochondria have exhibited "exceptional" sensitivity to copper accumulation due to direct damage of protein thiols, there is little support that redox modification of protein thiols is the reason for hepatotoxicity in WD. To date, there is a significant relationship between the decrease of total thiol or sulfhydryl groups in mitochondria and accumulated copper in mitochondria. Usually, this copper dependent damage is alleviated by chelating excess copper. This suggests that protein thiols, free thiols and/or glutathione are a direct target of copper ions and are likely a key factor in copper mediate cellular and mitochondrial damage. We propose that in hepatocytes there is a copper mediated attack of protein thiols thus leading to increased susceptibility to damage in mitochondria and ultimately cell death. The results of this study suggest a need for an increased study on the oxidation of mitochondrial protein thiols in WD.

Introduction

Wilson disease (WD) also known as “hepatolenticular degeneration” was first described in 1912 [1]. Patients with WD have a liver severely affected by excessive copper deposition. This results in serious clinical manifestations such as inefficient liver function, chronic hepatitis, or cirrhosis [2]. Excessive amounts of accumulated intracellular copper have been shown to induce oxidative stress to protein thiols by assuming “Fenton like " mechanisms or copper catalyzed oxidation which produces highly reactive radicals from hydrogen peroxide [3]. Accumulated copper has been noted to significantly contribute to mitochondrial damage by several mechanisms including dysregulation of lipids [4] in addition to oxidation of protein thiols [5]. Recently, studies have indicated a Fenton-like reaction happens in late stages of copper induced oxidative stress [6, 7]. Isolated mitochondria showed ultrastructural alteration such as swelling of intermembrane space when assessed by electron microscopy. These changes were a consequence of multiprotein crosslinking, reversible by copper-chelating therapies such as D-penicillamine and trientine [6]. Copper induced damage may follow a classical mechanism for protein damage by direct attack of target amino acid residues such as cysteine and methionine [8]. This targeted attack has the possibility of inducing conformational changes that can lead to activity loss of critical proteins [9]. Potential observed alterations to protein thiols that can occur from oxidative stress include formation of mixed disulfides or internal disulfides from vicinal dithiols, S-nitrosation of thiol groups, and the formation of higher oxidation states such as sulfenic, sulfinic, or sulfonic acids [10]. Why protein thiols or sulfhydryl related proteins are a direct target in copper toxicity has not been definitively described. It was once proposed that glutathione transported copper into mitochondrial IMS or mitochondrial matrix [11]. This idea was negated in findings where yeast with depleted levels of glutathione had wild-type

mitochondrial copper levels [12]. There is still evidence that glutathione may indirectly regulate or participate in mitochondrial copper homeostasis due to the redox state of cysteine sulfurs being important for proper copper binding of many proteins in mitochondria [13, 14, 15]. There is still much investigation needed to identify protein modifications specific to copper toxicity. In agreement with established findings, we aimed to determine if cellular thiols and related proteins that rely on thiol interactions were a target for copper ions during copper accumulation. We propose that protein thiols are primary targets for copper toxicity likely due to Fenton-like attacks to mitochondrial proteins. This in turn contributes to reduced mitochondrial function and membrane integrity.

Materials and Methods

Yeast Strains, Culture Conditions, and Standard Methods

The yeast strains used in this study were BY4741. All cultures were grown in YP (1% yeast extract, 2% peptone) medium or synthetic defined media (with selective amino acids excluded) with added filtered sterilized glucose. All the growth tests were performed at 30°C with 1:10 serial dilutions of pre-cultures grown in Yeast Extract Peptone Dextrose (YPD) at 30°C. Metal concentrations reported were achieved by adding exogenous metals ($CuSO_4$, $FeSO_4$) to the YPD media of the cultures for 48 hours prior to testing. Spot test growth conditions were measured using ImageJ software. Using ImageJ software, images of growth test plates were converted to binary images by selecting Process → Binary → Make Binary. Measurements of the binary image were taken measuring the area of each row of serial dilutions. The area was surrounded with a perimeter using an area selection tool. After the area was selected Analyze → Measure was used to transfer the measurement to a data collection window.

Mammalian Cell Culture Conditions

Human Embryonic Kidney (HEK 293) and Chinese Hamster Ovary (CHO) cells were cultured in Dulbecco's Modified Eagle Medium (DMEM) high glucose supplemented with 10% FBS, 1% L-uridine, 1% sodium pyruvate and 1% mercaptoethanol. The cells were maintained at 37 °C in a humidified atmosphere with 5% CO^2. For copper challenge experiments, cells were incubated for 48 h with 200 μM or 1000 μM copper histidine (CuHis). Concentrations chosen are comparable to copper concentrations found in brains of Wilson disease patients (ranging from 297 μM to 1092 μM) [5, 16].

Cytochrome C Oxidase (COX) Activity Assay

COX and Malate Dehydrogenase (MDH) activity were measured using a Shimadzu UV-2450. For COX activity assay cells were harvested after 48 hours of treatment and measured on parameters as previously described [12]. Malate dehydrogenase activity was determined by measuring the decrease in absorbance at 340 nm in reaction with added NADH [17]. Each sample was run in technical replicates of 3, measurements from each of those replicates were taken and the mean value was calculated for the experimental reading. Averages of COX activity was normalized to averages of MDH activity for a measurement of COX activity.

JC-1 microplate assay

Mitochondrial membrane potential ($\Delta\Psi m$) was assessed by means of the fluorescent cationic dye JC-1. Cells were washed with Phosphate Buffer Saline (PBS) solution and incubated with JC-1 (1 mg/ml) in suspension at a final concentration of 2 µM for 30 minutes at 30˚C and analyzed by a Cytation 5 Biotek microplate reader at 535 ex, 595 em wavelengths for aggregate fluorescence intensity and 485 ex, 535 em wavelengths for monomer fluorescence intensity.

JC-1 flow cytometry

Mitochondrial membrane potential ($\Delta\Psi m$) was assessed by the fluorescent cationic dye JC-1. Cells were washed with Phosphate Buffer Saline (PBS) solution and incubated with JC-1 (1 mg/ml) in suspension at a final concentration of 2 µM for 30 minutes at 30°C and analyzed by flow cytometry. Aggregates were detected using the PE channel and monomers were detected using the FITC channel.

Direct colorimetric assay for thiol and disulfide groups

Cells were homogenized in a cold assay buffer (100 mM Tris-HCl, pH 7.5 containing 1 mM EDTA. Fifty microliters (µl) of supernatant and 50 µl of fluorometric thiol detector DTNB (5,5'-dithio-bis-2-(nitrobenzoic acid)) and incubated at room temperature for five minutes in a black clear bottom 96-well plate. The 96-well plate was then transferred to a Cytation 5 Biotek microplate reader and read at an absorbance of 412 nm. Total cellular thiol concentration was calculated using an equation from the linear regression of a cysteine standard curve, substituting fluorescence values for each sample. [18, 19].

Serial dilution growth test

S. cerevisiae were grown in 5 ml YPD or synthetic complete glucose media to mid-exponential phase. Two hundred microliters (µl) of these cultures were transferred into a 96-well plate and diluted in sterilized deionized water as a 1:10 dilution for 5 times, each with a total volume of 200 µl. Five microliters (µl) of each dilution sample were tested on YPD media agar or synthetic complete glucose media agar. Media agar plates were grown for 24 hours at 30°C before measurement using ImageJ software.

Statistical Methodology

ANOVA

The one-way analysis of variance (ANOVA) was used to determine whether there were any significant differences between the means of three or more independent (unrelated) groups. In all ANOVAs shown, the variables were varying metal concentrations (copper). Statistical significance of variance between the means of the populations in question for each experiment were measured using the p-value. P values <0.05 were taken as indications of strong evidence against the null hypothesis.

Miscellaneous Methods

Aconitase activity was assayed by an aconitase activity kit purchased from Abcam (cat. no. ab109712). Protein concentrations were determined by the method of Bradford [20]. Quantification of spot intensity in serial dilution growth tests was performed using IMAGEJ software [21]. Scanned color images were converted to grayscale then to binary using the automated routine: Process-Binary-Make binary. The rectangular selection tool was used to specify the area of interest and measured. Interference of copper/GSH was not considered in any experimental settings.

Results

Dose dependent copper toxicity in *Saccharomyces cerevisiae*

High amounts of copper can be detrimental to cellular processes and growth. To investigate the amount of copper required to inhibit the growth of *Saccharomyces cerevisiae* (BY4741 strain) we plated cells on rich medium with fermentable carbon source with increasing copper in the form of Cu-sulfate salt. The wild-type yeast strain showed a growth defect in the presence of 8 mM exogenous copper added to growth media (Figure 2.1A, Figure 2.1B). No change in growth was observed at concentration below 8 mM (data not shown).

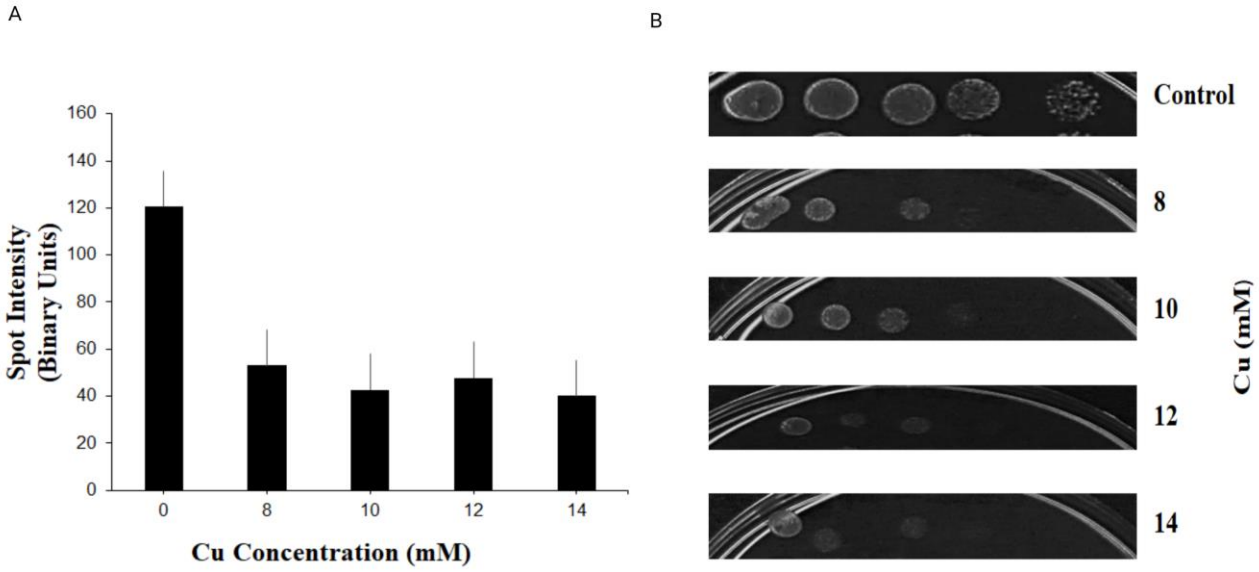

Figure 2.1 Serial dilutions of WT BY4741

A) Spot intensity was measured by converting the scanned color images of selected plates to binary images. Measurements of the binary pixels within a selected area were measured for spot intensity (pixel density) using IMAGEJ software. Three separate biological replicates were measured, averaged, and plotted (n=3). Error bars shown represent the standard error. B) Yeast strain BY4741 was serially diluted and plated onto YPD agar plates containing varying concentrations of $CuSO_4$. Pictured is one chosen image of three biological replicates. You need to make this an appendix to the chapter and take the results of the ANOVA and put it in the figure legend of each experiment. A p-value of 9.70129E-0.5 was obtained from a one-way ANOVA.

Mitochondrial membrane potential (ΔΨm) is compromised by copper

To test mitochondrial function during copper accumulation, we determined mitochondrial membrane potential (ΔΨm) in Chinese Hamster Ovary (CHO) cells by staining with the cationic dye JC-1. JC-1 fluoresces red or green, to indicate aggregates or monomers, respectively. A high number of monomers indicates dysfunctional mitochondria with lower ΔΨm, in comparison an increased number of aggregates indicates healthy mitochondria with higher ΔΨm. In flow cytometry ΔΨm is assessed by monitoring the populations movement across the x-axis (PE-A) and y-axis (FITC). Increasing FITC signal fluorescence corresponds to increasing monomers (movement up the y axis) and increasing PE-A signal fluorescence corresponds to increasing aggregates (movement to the right of the x axis). JC-1 accumulation in CHO cells cultured in different copper concentrations (supplied as copper-histidine complex) is shown in green/orange bivariate plots (Figure 2.2). These plots show increased level of monomers with copper treatment suggests a loss of ΔΨm. We observed a dramatic increased level of monomer at the highest concentration of copper (Figure 2.2E) when compared to control groups and low copper concentration treated groups. (Figure 2.2C and Figure 2.2D).

To confirm the loss of ΔΨm the assay was performed in *S. cerevisiae*, JC-1 was stained using the same concentrations and analyzed by microplate assay with 535 ex, 595 em wavelengths for aggregate fluorescence intensity and 485 ex, 535 em wavelengths for monomer fluorescence intensity. In agreement with the flow cytometry data, yeast treated with copper sulfate showed a dose dependent increase in monomers. A decreased ratio indicates increasing values of the denominator (monomers) and decreasing or non-changing value of the numerator (aggregates). A decreased ratio was seen in yeast treated with high copper concentrations when compared with control groups in the experiment (data not shown).

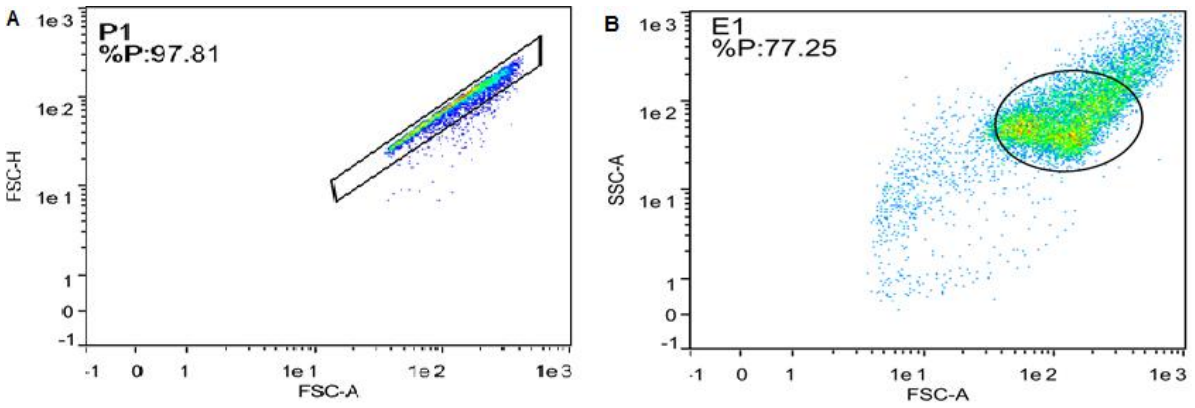

Population	% Par.
E1 [Control+JC-1]	77.25
P1 [Control+JC-1]	97.81

Population	% Par.
Control+JC-1	100.00
E1 [Control+JC-1]	77.25

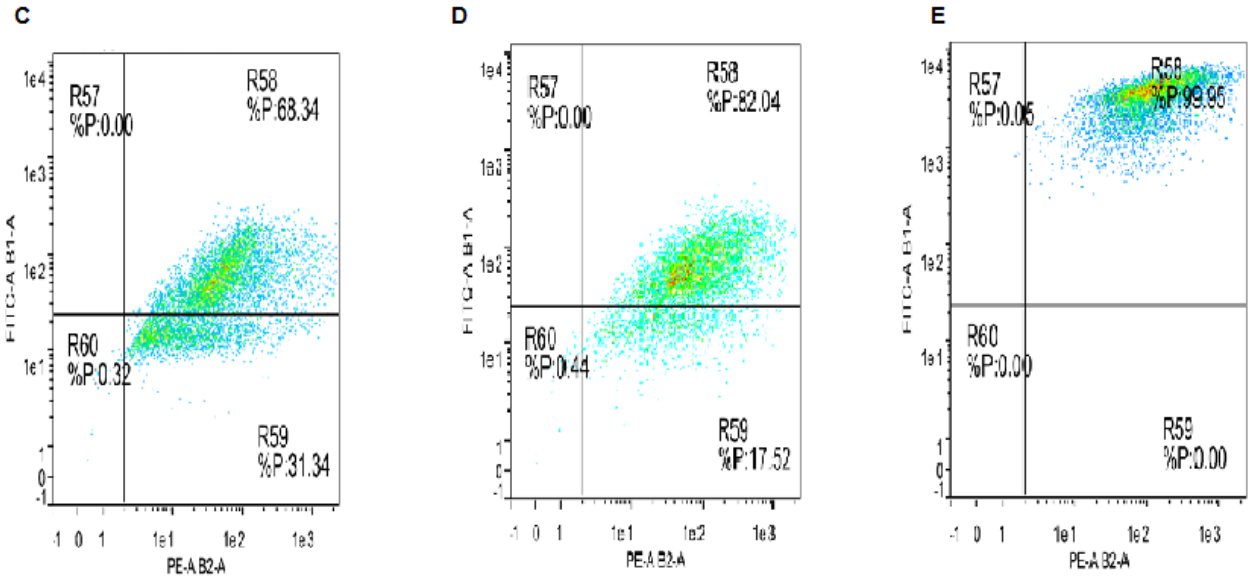

Figure 2.2 Flow cytometry analysis of CHO cells

JC-1 accumulation in CHO cells reflected in green (FITC)/orange (PE-A) plots (A&B). Flow cytometry analysis of CHO cells included treatment with copper histidine at concentrations of 200 (C), 600 (D), and 1000(E) µM. Harvested cells were stained in suspension with JC-1 in suspension at a final concentration of 2 µM and incubated for 30 minutes at 37 °C, 5% CO_2. Results were reported in green (FITC)/orange (PE-A) bivariate plots.

Copper toxicity leads to decreased cytochrome *c* oxidase activity

To test the effects of copper accumulation on biochemical processes in mitochondria we assessed cytochrome *c* oxidase (COX) activity. Oxidation of cytochrome *c* oxidase is measured at 550 nm monitoring the conversion of reduced cytochrome c to oxidation based on the Soret bands of the cytochrome. As a control malate dehydrogenase (MDH) activity was measured in the direction of NADH-dependent reduction of oxaloacetate measuring the decrease in absorbance at 340 nm. The ratio of COX/MDH controls for the number of mitochondria and any treatment effects on activity. HEK293 cells treated with exogenous copper histidine show a dose dependent decrease in COX activity relative to the untreated cells (Figure 2.3)

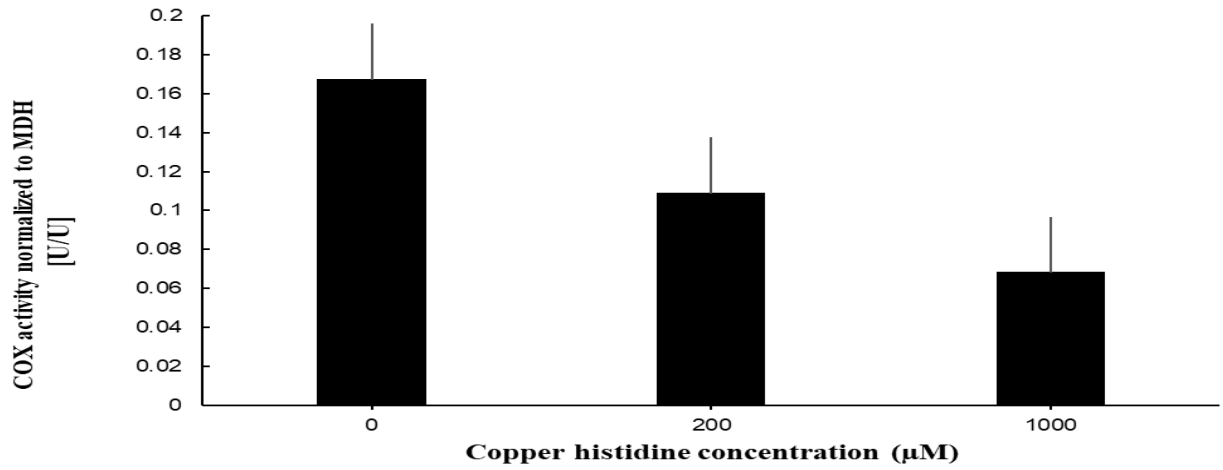

Figure 2.3 COX activity assay of HEK 293 cells

HEK 293 cells were harvested by centrifugation and washed in a PBS buffer. Harvested samples were used for both COX and MDH enzymatic activity. Oxidation of cytochrome c oxidase is measured at 550 nm. MDH activity was measured in the direction of NADH-dependent reduction of oxaloacetate. The reaction was followed by measuring the decrease in absorbance at 340 nm. Experimental readings were run in triplicate. The graph represents the average of three separate experiments. Error bars shown represent the standard error. A p-value of 0.88646 was obtained from a one-way ANOVA.

Aconitase activity during copper accumulation

To assess the activity of Fe-S proteins in response to copper overload we measured aconitase activity using a time-resolved fluorescence technique. Mitochondrial aconitase is a reversible enzyme that catalyzes the conversion of citrate to isocitrate [21]. Because aconitase contains a [4Fe-4s] cluster [21] we use aconitase activity to indirectly assess copper's effect on Fe-S cluster production in mitochondria. Here, aconitase activity was measured in HEK 293 cells. The activity measurement suggested a decrease in activity at 1000 μM copper histidine however this difference was not statistically significant ($p=0.208983$). This result is not consistent with previous findings that show aconitase as a sensitive measure of toxicity and these concentrations appear to be toxic therefore further investigation to increase sample size is required.

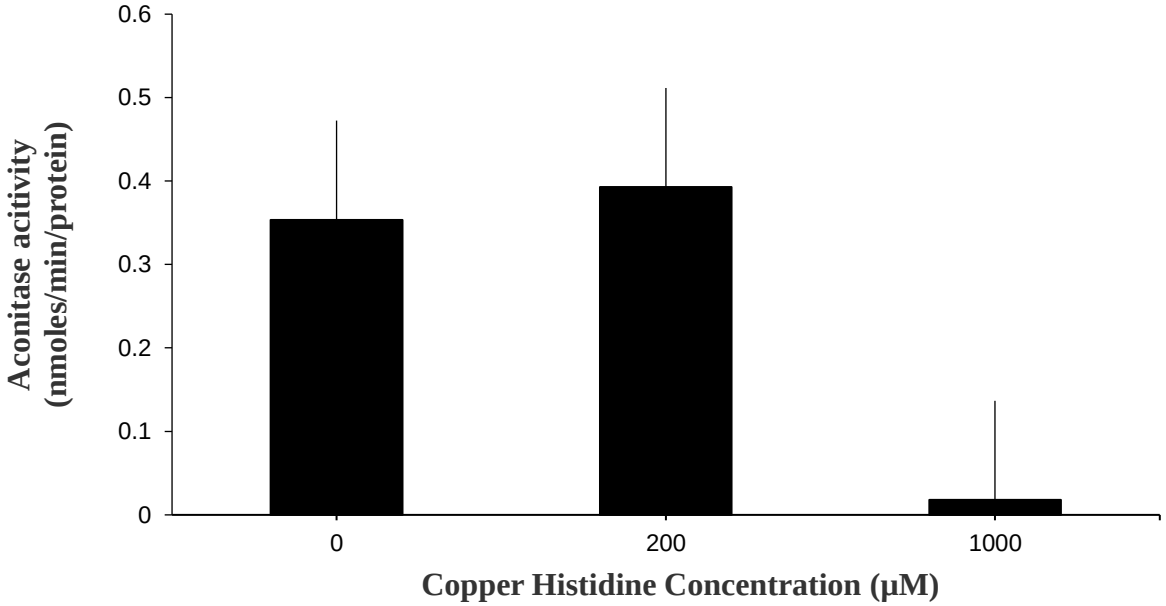

Figure 2.4 Aconitase activity in HEK 293

Aconitase activity in response to added exogenous copper in HEK 293 cells. Aconitase assay activity kit and protocol were performed as previously described by Abcam (cat. no. ab109712). Time resolved fluorescence and enzymatic activity was graphed as a function of nmoles per minute per protein. A p-value of 0.219812 was obtained from a one-way ANOVA.

Total cellular thiols decrease in response to increasing added copper

To assess cellular total cellular sulfhydryl concentration an Ellman's assay [23] was performed in HEK293 cells (Figure 2.6A) and *S. cerevisiae* (Figure 2.6B). 5,5'-Dithio-bis (2-nitrobenzoic acid) was used as a fluorometric detector of cellular thiols levels. It should be that this analysis represents levels of total cellular thiols and does not specify the form of thiols detected e.g., Glutathione versus protein thiols. We observe a weak negative correlation between copper concentration and total thiol concentration in HEK293 but not in yeast.

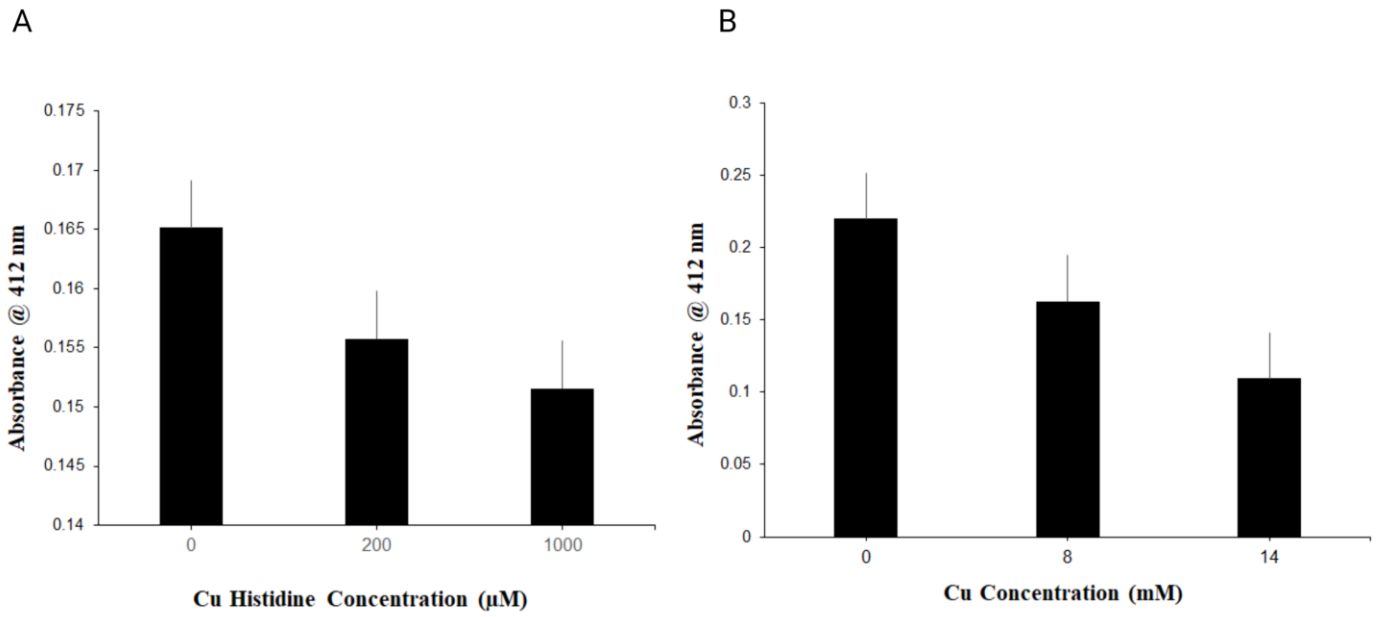

Figure 2.5 Ellman's assay using (Ellman's reagent) 5,5'-Dithio-bis (2-nitrobenzoic acid) in *Saccharomyces cerevisiae* and HEK 293

A) Total thiol concentration of HEK 293 cells with copper histidine treatment of 0, 200 and 1000 µM, respectively. Error bars pictured represent the standard error. n=3 B) Total thiol concentration of *S. cerevisiae* cells with copper sulfate treatment of 0, 8 and 14 mM, respectively. In both groups the optical absorbance extinction was measured at 412 nm. Total cellular thiol concentration was estimated from sample ODs using a calibration curve of ODs as function of standard (Acetylcysteine) concentrations. Error bars pictured represent the standard error. A p-value of 0.219812 and 0.0752925 was obtained from a one-way ANOVA, respectively. n=3

Results of Analysis of Variance (ANOVA)/ Multiple Comparisons Test

To determine if there were significant differences between the groups of each experiment a one-way ANOVA was used. The p- value is used to determine statistical significance. If $P < 0.05$ then sample results are deemed statistically significant and thus the null hypothesis is rejected. For the analyses below the P value is 0.05. P values <0.05 were taken as indications of strong evidence against the null hypothesis (H_0). Where H_0 is μcontrol = μexperimental and there is no difference in means. If the p-value indicated that the data was statistically significant, pairwise post-hoc testing was performed to determine whether there was a difference between all possible pairs using studentized range distribution [24].

Table 2.1 Copper and *S. cerevisiae* ANOVA

Source of Variation	SS	df	MS	F	P-value	F crit
Between Groups	13675.07	4	3418.767	19.76754	9.70129E-05	3.47805
Within Groups	1729.485	10	172.9485			
Total	15404.55	14				

The p-value is less than the assigned significance level 0.05. Thus, we reject the null hypothesis and state that the result is statistically significant. n=3

Table 2.2 Tukey's multiple comparison test (Copper and SA)

Tukey's multiple comparisons test	Mean Diff.	95.00% CI of diff.	Below threshold?	Summary	Adjusted P Value	
Control vs. 8 mM Cu	67.46	32.13 to 102.8	Yes	***	0.0007	A-B
Control vs. 10 mM Cu	77.9	42.56 to 113.2	Yes	***	0.0002	A-C
Control vs. 12 mM Cu	72.78	37.44 to 108.1	Yes	***	0.0004	A-D
Control vs. 14 mM Cu	80.48	45.14 to 115.8	Yes	***	0.0002	A-E
8 mM Cu vs. 10 mM Cu	10.43	-24.91 to 45.77	No	ns	0.8619	B-C
8 mM Cu vs. 12 mM Cu	5.312	-30.03 to 40.65	No	ns	0.9861	B-D
8 mM Cu vs. 14 mM Cu	13.02	-22.32 to 48.36	No	ns	0.7451	B-E
10 mM Cu vs. 12 mM Cu	-5.12	-40.46 to 30.22	No	ns	0.9878	C-D
10 mM Cu vs. 14 mM Cu	2.586	-32.75 to 37.92	No	ns	0.9991	C-E
12 mM Cu vs. 14 mM Cu	7.706	-27.63 to 43.04	No	ns	0.9476	D-E

A Tukey-Kramer post-hoc test was used to compare the population's means of *S. cerevisiae* growth in response to added copper to growth medium. Absolute mean difference between each group was found using the averages listed in the ANOVA output, studentized Range Q Table was used to find the Q value and lastly absolute mean difference was measured between each group to the critical Q value. If the absolute mean difference is greater than the Q critical value, then the difference between the group averages is statistically significant. For this test we found that only the difference in means in the following groups were statistically significant: A and B, A and C, A and D, and A and E.

Table 2.3 COX activity assay ANOVA

Source of Variation	SS	df	MS	F	**P-value**	F crit
Between Groups	0.015226	1	0.015226	4.121489	**0.088646**	5.987378
Within Groups	0.022166	6	0.003694			
Total	0.037392	7				

The p-value is greater than the assigned significance level 0.05. Thus, we cannot reject the null hypothesis and cannot confirm complete statistical significance. We do conclude a trend towards significance n=3.

Table 2.4 Aconitase activity assay ANOVA

Source of Variation	SS	df	MS	F	**P-value**	F crit
Between Groups	0.049055	1	0.049055	2.238043	**0.208983**	7.708647
Within Groups	0.087676	4	0.021919			
Total	0.136731	5				

The p-value is greater than the assigned significance level 0.05. Thus, we fail to reject the null hypothesis and state that the result is not statistically significant. n=4

Table 2.5 Ellman's assay in S. cerevisiae ANOVA

Source of Variation	SS	df	MS	F	**P-value**	F crit
Between Groups	0.000581	2	0.000291	1.678836	**0.219812**	3.68232
Within Groups	0.002596	15	0.000173			
Total	0.003177	17				

The p-value is greater than the assigned significance level 0.05. Thus, we cannot reject the null hypothesis and cannot confirm complete statistical significance. We do conclude a trend towards significance n=3.

Table 2.6 Ellman's assay in HEK 293 ANOVA

Source of Variation	SS	df	MS	F	**P-value**	F crit
Between Groups	0.012214	2	0.006107	6.912469	**0.075292**	9.552094
Within Groups	0.002651	3	0.000884			
Total	0.014865	5				

The p-value is greater than the assigned significance level 0.05. Thus, we cannot reject the null hypothesis and cannot confirm complete statistical significance. We do conclude a trend towards significance n=3.

Discussion

Wilson Disease (WD) patients and animal models have impaired copper excretion from the liver which leads to copper accumulation. These patients and animal models show mitochondrial destruction due to the progressive, dose-dependent damage due to copper overload. In this chapter we present data for modelling these copper dependent defects, including a decrease in cellular thiols. Oxidative stress is currently accepted to be the causative agent in many diseases. In WD it is thought that this oxidative stress, induced by an accumulation of copper, results in direct attacks of cellular and mitochondrial protein thiols [3, 5, 25, 26]. Most thiols that exist in mitochondria are in the mitochondrial matrix, which protect against oxidative damage by forming protein-protein disulfides and mixed disulfides with glutathione [25]. Oxidation of mitochondrial matrix protein thiols may cause a subsequent decrease in mitochondrial protein functionality. Here we report an inverse relationship between the concentration of cellular thiols and increased exogenous copper levels in HEK293 cells. Though we observe a decrease in *S. cerevisiae*, we need further testing to solidify a relationship of the two in yeast. From this result we conclude that either in yeast thiols are not susceptible to direct attack by unbound copper ions or that the sample size needs to be increased to generate statistical significance.

In yeast the thiol containing compound glutathione plays a significant role in Fe-S assembly and distribution. The most notable phenotype for *S. cerevisiae* mutants depleted of glutathione is inefficient Fe-S cluster assembly [28]. Aconitase is an Fe-S enzyme involved in the Krebs's cycle. Here we assess Fe-S cluster assembly by measuring aconitase activity. There is no significant correlation between increased copper levels and aconitase activity in mammalian cells as tested. Our data does not support that glutathione is specifically affected.

Though previous published results from other groups have identified cellular thiols as a target of copper, therefore more investigation into which thiols are oxidized by copper overload is.

Cytochrome c oxidase (COX) does exhibit a decrease in function as copper levels increase in the cell. Bovine heart cytochrome c oxidase contains 14-16 cysteine residues in its structure [29]. Since these residues are not buried in the core of the enzyme, they can be easily oxidized by ROS created by unbound copper ions. In this study observe a copper dependent decrease in cytochrome c oxidase activity. It is unclear if this is due to oxidation of the thiols or structural damage to membranes or a combination.

To demonstrate a phenotypic outcome is not restricted to COX or ETC function we performed an experiment with fermenting *S. cerevisiae.* While fermenting yeast does not need COX yet copper can still be toxic. To supplement this data and assess the effects of copper accumulation in this study we measured $\Delta\Psi m$ using the cationic dye JC-1. Lowered membrane potential can be an indicator of organelle damage [5]. Here we report mitochondrial damage in response to increasing amounts of copper in both CHO cells and *S. cerevisiae*. This is in agreeance with findings by Borchard et al [5] that showed significant membrane damage because of copper accumulation. Thus, we suspect that copper overload in mitochondria is causing the same modifications to the mitochondrial membrane and related mitochondrial membrane proteins possibly by attack on cellular thiols. More studies are needed to identify where and what thiols or thiol containing proteins are specifically affected during copper accumulation. We cannot state there is a Fenton-like chemistry occurring during mitochondrial and cellular damage when copper accumulates as our attempts to detect increased ROS with assays such as dihydroethidium staining does not yield statistically significant results (data not shown).

One possible mechanism of copper toxic would be disruption of mitochondria protein import. The translocase of the outer membrane (TOM) complex mediates the import of the mitochondria protein precursors and is the general import machinery for mitochondrial proteins. The TOM components exposed to the cytosol—Tom20 and Tom70—function as receptors with hydrophilic domains exposed to the cytosol [30, 31]. Although Tom20 and Tom70 are the main receptors, Tom22, which connects Tom20 to the pore of the TOM complex, also has a role in the later stages of translocation from the OM to the IM [32]. For transport into the mitochondrial matrix glutathione must pass through the porins of the outer mitochondrial membrane (OMM) and TOM [33]. Recently scientists have found that the porin Por1 binds to newly imported Tom22. Thereby Por1 modulates the incorporation of Tom22 into the TOM complex [34]. The glutathione pool of the IMS is in equilibrium with the cytosolic glutathione pool because of the presence of porins that allow free passage of reduced glutathione (GSH) and oxidized glutathione (GSSG) across the outer mitochondrial membrane [35]. It is possible that excess copper in the cytosol of a cell interferes with protein machinery of the TOM complex, ultimately disrupting the import of GSH to the IMS. In this hypothesis, GSH is prematurely oxidized by free copper ions and is not recognized by either Por1 or Tom22. Confirming this mechanism would involve studying the effects of TOM22 expression, or lack thereof, on total cellular and mitochondrial sulfhydryl groups, mitochondrial dysfunction and structure, mitochondrial membrane potential and ATP synthesis. Glutathione deficiency has been implicated in the pathogenesis of many diseases including liver disease, Parkinson's disease, cancer, and HIV/AIDS [36]. Studies on dysregulation of glutathione metabolism and homeostasis in Wilson Disease are limited. Furthermore, no connections in the TOM complex and Wilson Disease have

been made to date. Increasing implications for glutathione metabolism will increase the understanding of pathology and molecular biology for WD.

Mitochondrial copper homeostasis continues to remain largely a mystery that needs much future investigation. Understanding the defense system against metal toxicity in mitochondria could prove useful for advances in diseases such as WD. To solidify the relationship of copper-dependent attacks and thiols we will focus on studies that assess this in further detail in both yeast and mammalian cells. If a Fenton-like chemistry cannot be concretely established, a pinpoint of where the attacks happen (i.e., in transport or in late stages due to accumulation in the matrix) would prove useful. Fenton reactions pin harmful reactive oxygen species as the cause rather than the effect. To prove Fenton chemistry, an elevated amount of hydroxyl radicals would have to be observed prior to significant protein damage. Dose dependent emergence of reactive oxygen species in response to copper exposure should be studied.

References

1. Wilson, S. A. K. (1912) Progressive lenticular degeneration: A familial nervous disease associated with cirrhosis of liver. *Brain*, 34, 295-507.
2. Beinhardt S., Leiss W., Stättermayer A. F., Graziadei I., Zoller H., Stauber R., Maieron A., Datz C., Steindl-Munda P., Hofer H., Vogel W., Trauner M., Ferenci P. (2014) Long-term outcomes of patients with Wilson disease in a large Austrian cohort. *Clin. Gastroenterol. Hapatol.* 12, 683-689.
3. Sokol, R. J., Twedt, D., McKim, J. M., Jr, Devereaux, M. W., Karrer, F. M., Kam, I., von Steigman, G., Narkewicz, M. R., Bacon, B. R., Britton, R. S. (1994). Oxidant injury to hepatic mitochondria in patients with Wilson's disease and Bedlington terriers with copper toxicosis. *Gastroenterology*, 107, 1788–1798.
4. Sauer, S. W., Merle, U., Opp, S., Haas, D., Hoffmann, G. F., Stremmel, W., Okun, J. G. (2011) Severe dysfunction of respiratory chain and cholesterol metabolism in Atp7b (-/-) mice as a model for Wilson disease. *Biochimica et biophysica acta*, 1812, 1607–1615
5. Borchard, S., Bork, F., Rieder, T., Eberhagen, C., Popper, B., Lichtmannegger, J., Schmitt, S., Adamski, J., Klingenspor, M., Weiss, K. H., Zischka, H. (2018) The exceptional sensitivity of brain mitochondria to copper. *Toxicology in vitro: an international journal published in association with BIBRA*, 51, 11–22.
6. Zischka, H., Lichtmannegger, J., Schmitt, S., Jägemann, N., Schulz, S., Wartini, D., Jennen, L., Rust, C., Larochette, N., Galluzzi, L., Chajes, V., Bandow, N., Gilles, V. S., DiSpirito, A. A., Esposito, I., Goettlicher, M., Summer, K. H., Kroemer, G. (2011) Liver mitochondrial membrane crosslinking and destruction in a rat model of Wilson disease. *The Journal of clinical investigation*, 12, 1508–1518
7. Huster D. (2014) Structural and metabolic changes in Atp7b-/- mouse liver and potential for new interventions in Wilson's disease. *Annals of the New York Academy of Sciences*, 1315, 37–44.
8. Davies M. J. (2016) Protein oxidation and peroxidation. *The Biochemical journal*, 473, 805–825
9. Mirzaei, H., Regnier, F. (2006) Creation of allotypic active sites during oxidative stress. *Journal of proteome research*, 5, 2159–2168.
10. Stamler, J. S., Hausladen, A. (1998) Oxidative modifications in nitrosative stress. *Nature structural biology*, 5, 247–249.
11. Marí, M., Morales, A., Colell, A., García-Ruiz, C., & Fernández-Checa, J. C. (2009) Mitochondrial glutathione, a key survival antioxidant. *Antioxidants & redox signaling*, 11, 2685–2700.
12. Cobine, P. A., Ojeda, L. D., Rigby, K. M., Winge, D. R. (2004) Yeast contain a non-proteinaceous pool of copper in the mitochondrial matrix. *The Journal of biological chemistry*, 279, 14447-14455.
13. Zischka, H., Finer, C., (2018) Mitochondrial copper homeostasis and its derailment in Wilson disease. *The International Journal of Biochemistry & Cell Biology*, 102, 71-75.
14. Leary, S. C., Sasarman, F., Nishimura, T., Shoubridge, E. A. (2009) Human SCO2 is required for the synthesis of CO II and as a thiol-disulphide oxidoreductase for SCO1. *Human molecular genetics*, 18, 2230–2240.
15. Banci, L., Bertini, I., Ciofi-Baffoni, S., Hadjiloi, T., Martinelli, M., Palumaa, P. (2008) Mitochondrial copper(I) transfer from Cox17 to Sco1 is coupled to electron

transfer. *Proceedings of the National Academy of Sciences of the United States of America*, 105, 6803–6808.
16. Lai, J. C., Blass, J. P. (1984) Neurotoxic effects of copper: inhibition of glycolysis and glycolytic enzymes. *Neurochemical research*, 9, 1699–1710.
17. Worthington Biochemical Company. n.d. Malate Dehydrogenase Assay. *Worthington Biochem.*
18. Chan, K., Wasserman, B. P. (1992) Direct Colorimetric Assay of Free Thiol Groups and Disulfide *Cereal chemistry*, 70, 22-6
19. Chemical, Cayman. n.d. Thiol Assay Detection Kit. *Cayman chemical.*
20. Bradford M. M. (1976) A rapid and sensitive method for the quantitation of microgram quantities of protein utilizing the principle of protein-dye binding. *Analytical biochemistry*, 72, 248–254.
21. Rasband, W.S. (1997-2016) *Image J. U.S. National Institute of* Health, Bethesda, Maryland, USA..
22. Quirós P. M. (2018) Determination of Aconitase Activity: A Substrate of the Mitochondrial Lon Protease. *Methods in molecular biology (Clifton, N.J.)*, 1731, 49–56.
23. Ellman, G. L. (1959) Tissue sulfhydryl groups. *Arch Biochem Biophys*, 82,70-77.
24. Dubitzky, W., Wolkenhauer, O., Cho, K. H., Yokota, H. (2013) Tukey–Kramer Method. Encyclopedia of Systems Biology
25. Liu, S.S. (1997) Generating, partitioning, targeting and functioning of superoxide in mitochondria. *Bioscience. reports.*17, 259–272.
26. Tan, S., Sagara, Y., Liu, Y., Maher, P., Schubert, D. (1998). The regulation of reactive oxygen species production during programmed cell death. *The Journal of cell biology*, 141, 1423–1432.
27. Coulter, C. V., Kelso, G. F., Lin, T. K., Smith, R. A., Murphy, M. P. (2000). Mitochondrially targeted antioxidants and thiol reagents. *Free radical biology & medicine*, 28, 1547–1554.
28. Sipos, K., Lange, H., Fekete, Z., Ullmann, P., Lill, R., Kispal, G. (2002) Maturation of cytosolic iron-sulfur proteins requires glutathione. *The Journal of biological chemistry*, 277, 26944–26949.
29. Verheul, F. E., Draijer, J. W., Muijsers, A. O., Van Gelder, B. F. (1982) The reactivity of thiol groups in bovine heart cytochrome c oxidase towards 5,5'-dithiobis(2-nitrobenzoic acid). *Biochimica et biophysica acta*, 681, 118–129.
30. Maryon, E. B., Molloy, S. A., Kaplan, J. H. (2013). Cellular glutathione plays a key role in copper uptake mediated by human copper transporter 1. *American journal of physiology. Cell physiology*, 304, C768–C779.
31. MacPherson, L., & Tokatlidis, K. (2017). Protein trafficking in the mitochondrial intermembrane space: mechanisms and links to human disease. *The Biochemical journal*, 474, 2533–2545.
32. Rapaport D. (2002). Biogenesis of the mitochondrial TOM complex. *Trends in biochemical sciences*, 27, 191–197.
33. Hewitt, V., Lithgow, T., Waller, R.F. (2014) Modifications and Innovations in the evolution of mitochondrial protein import pathways. *Endosymbiosis*, 19–35.
34. Brix, J., Dietmeier, K., Pfanner, N. (1997) Differential recognition of preproteins by the purified cytosolic domains of the mitochondrial import receptors Tom20, Tom22, and Tom70. *The Journal of biological chemistry*, 272, 20730–20735.

35. Kojer, K., Bien, M., Gangel, H., Morgan, B., Dick, T. P., Riemer, J. (2012) Glutathione redox potential in the mitochondrial intermembrane space is linked to the cytosol and impacts the Mia40 redox state. *The EMBO journal*, 31, 3169–3182.
36. Wu, G., Fang, Y. Z., Yang, S., Lupton, J. R., Turner, N. D. (2004) Glutathione metabolism and its implications for health. *The Journal of nutrition*, 134, 489–492.

Chapter 3
Copper dependent heme defect in *Saccharomyces cerevisiae*

Abstract

Most of the iron sequestered in the body is used for heme synthesis, Fe-S cluster proteins and other redox enzymes. Other metals such as Cu, Zn, Pb and Ga often compete with iron transport. This competition leads to a reduction in cellular iron pool causing negative clinical manifestations in human disease. Heme is important for cell survival and is required in multiple cellular pathways. Competition from other metals damages aspects of the heme synthesis pathway including gene expression, enzymatic activity, and iron integration into protoporphyrin IX (PPIX). The shared affinity of iron and other metals in certain proteins leads to an overlap of systems that traffic the metals within the cell and organelles including transport in Golgi apparatus, endoplasmic reticulum, and mitochondria. This overlap is a growing area of interest in human health in diseases where metal accumulation is a consequence such as Wilson Disease. Here, we demonstrate that a dose- dependent heme defect in yeast occurs in response to elevated exogenous copper. The phenotype was worsened with the addition of heme biosynthesis inhibitor, succinyl acetone or addition of supplemental oleic acid, ergosterol and methionine. The heme defect was partially alleviated by the deletion of transporter Mrs3. We propose here that the defect does not reflect damage to ferrochelatase but competition of binding for Mrs3. Accumulated copper is transported by Mrs3, ultimately inhibiting the synthesis of heme.

Introduction

Findings as early as 1922 from Lowy report excess storage of iron in the liver [1]. In the cell, mitochondria are the location of two processes important in iron metabolism: heme biosynthesis and Fe-S cluster synthesis [2]. Mitochondria are also equally important for the movement of copper ions. In *Saccharomyces cerevisiae*, Cu(I) enters the cell via low affinity and high affinity permeases [3]. One of the high affinity uptake systems is Ctr1. Once Cu(I) is inside the cell it is transported to one of the Cu(I)-binding metallochaperones, Atx1 [4]. Cu(I) then uses Atx1 as a vehicle for transport to the Ccc2 P-type ATPase located in the post-Golgi vesicles [5]. Atox1, the human ortholog to Atx1, transports copper ions to the homologous Menkes and Wilson P-type ATPases [6]. Both the Menkes and Wilson P-type ATPAs then transfer Cu(I) to secretory copper metalloenzymes Fet3 in yeast which is required for high affinity iron uptake [7]. Once iron enters the cell it is distributed to mitochondria by an unknown mechanism. Once at the mitochondria is transported to the matrix via Mrs3, Mrs4 and Rim2. Mrs3 and Mrs4, closely related proteins of the mitochondrial carrier family (MCF), that have established functions in mitochondrial iron homeostasis [8, 10, 11, 12]. Rim2 is another MCF which is shown to transport iron-nucleotide complexes. The combination of these proteins make iron available for both heme and Fe-S cluster assembly.

Heme biosynthesis starts with a rate-limiting step of the formation of δ-aminolevulinic acid (δ-ALA, 5-ALA or dALA) by the reaction of succinyl-coA with the amino acid glycine with succinyl-CoA, an intermediate of the Kreb's cycle. dALA is then combined by porphobilinogen synthase to give porphobilinogen, which has a pyrrole ring. Porphobilinogen is then hydrolyzed to form the tetrapyrrole, uroporphyrinogen III. Uroporphyrinogen undergoes many modifications, but in mammalians the most important modification produces a tetrapyrrole

protoporphyrin IX (PPIX). PPIX is combined with iron with the aid of enzyme ferrochelatase (FCH) to form heme [13]. In yeast ferrochelatiase is encoded by *HEM15* and a *Δhem15* strain has a heme defect. In this strain transcription of FET3 is induced showing the link between the final product and cellular accumulation of iron [2]. As Fet3 is a multicopper oxidase, copper-iron metabolism is linked and interaction between these metals in mitochondria is an increasing area of interest.

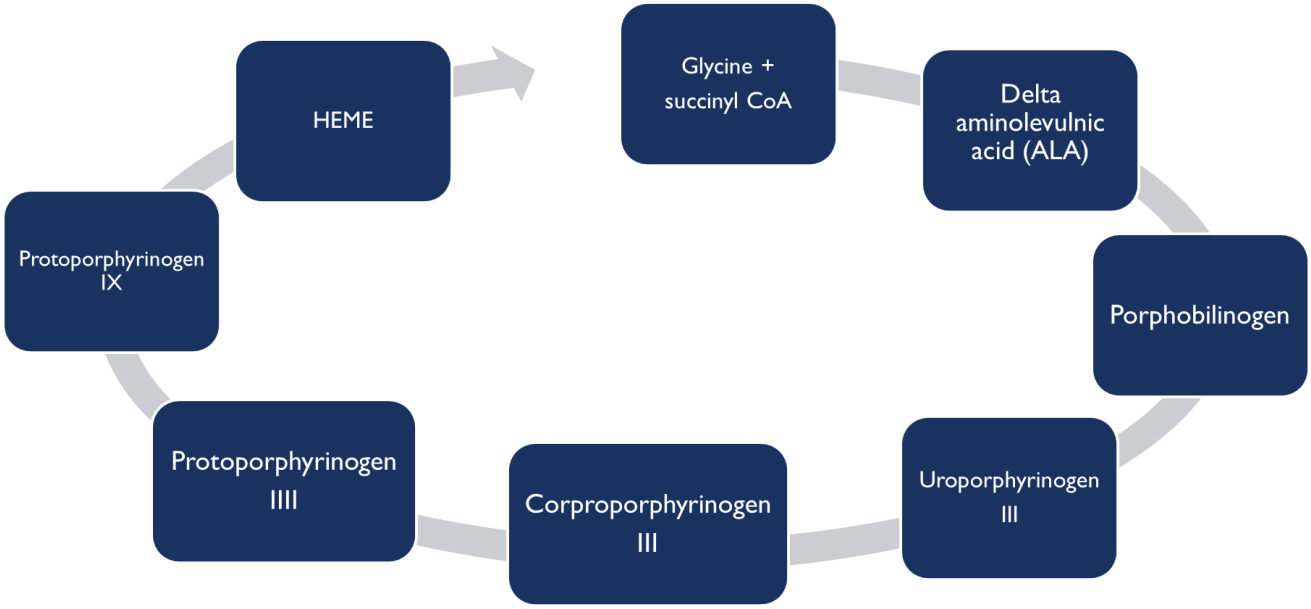

Figure 3.1. Heme biosynthesis pathway

Heme biosynthesis pathway in non-photosynthetic eukaryotes. This is the pathway of Heme B; modulators are not depicted. This depiction is general and does not include the enzymes involved between each step.

FCH has not only been named to catalyze the insertion of iron but more divalent transition metal ions such as zinc, nickel, cobalt, and copper. Substrate inhibition occurs in this order of affinity: $Cu^{2+} > Zn^{2+} > Co^{2+} > Ni^{2+}$ [14]. This can prove problematic when competing substrates accumulate in the cytosol or mitochondria in diseases, such as occurs in Wilson disease. Therefore, there is substantial preliminary evidence to believe that metals involved in substrate inhibition for the binding of ferrochelatase could be involved in the disruption of heme biosynthesis. Herein in this chapter we present a copper-dependent heme defect related to the *MRS3* gene in *S. cerevisiae* strain BY4741. Our results suggest that competing copper levels efficiently inhibit iron transport into the matrix by interfering with iron transport by Mrs3 which in turn lowers heme levels in a dose dependent manner. This defect does not seem to be due to competition for binding sites of ferrochelatase as no increase in PPIX is observed.

Materials and methods

Yeast strains, culture conditions, and standard methods.

Yeast strains used were WT BY4741 (Mrs3Δ, gsh1Δ, ccc2Δ, atx1Δ). Cultures were grown in 1% yeast extract, 2% peptone (YP) medium using glucose as a carbon source. Exogenous copper and iron were provided by adding $CuSO_4$ and $FeSO_4$, respectively. Growth tests were performed at 30 °C with 1:10 serial dilutions of overnight pre-cultures grown in YP plus 1% glucose.

Preparation of ergosterol/Tween 80/ methionine solution (TEM)

Ergosterol was added in a concentration of 2 mg/ml to 1:1 Tween 80 (purchased from Sigma-Aldrich, stock keeping no. P1754) and laboratory grade ethanol from Carolina (catalog item no. 861285). Methionine stock was purchased from VWR (catalog no. 97063-012) and used to make a 27.8 mg/ mL solution as described by Crisp et al. [2]. If added to YPD agar plates, the media was cooled before the TEM solution was added at 4% v/v.

Expression of Mrs3 in Lactococcus lactis

L. lactis cells were transformed with vector (pNZ8148) alone or pNZ8148 (MoBiTec) carrying the MRS3 gene were grown overnight at 30˚C in M17 medium with 0.5% glucose and 10 µg/mL chloramphenicol. Cells were diluted into fresh medium at an OD600 of 0.1, grown to an OD600 of 0.4, and induced using 1 ng/mL nisin for five hours as described by Vest et al. (2016)

Expression of recombinant protein

The MRS3 ORFs were cloned into pHis parallel 1. The fidelity of each construct was verified by dideoxynucleoside sequencing prior to use. *Escherichia coli* strain BL21 (DE3) cells were transformed with appropriate vectors and protein expression was induced for 3 hours. Inclusion bodies were isolated by the method described by Palmieri et al. [15]. Briefly, cells were resuspended in 1X potassium phosphate buffer (140 mM NaCl, 2.7 mM KCl, 8.3 mM KH_2PO_4,

1.8 mM KH_2PO_4), pH 7.5 and disrupted by sonication. Insoluble material was collected by centrifugation at 18,500 g. Insoluble material was resuspended in 1X potassium phosphate buffer, pH 7.5, and loaded onto a stepwise 40%, 53%, 70% sucrose gradient. Samples were centrifuged at 18,500 g for one hour and inclusion bodies were isolated as a gray colored band at the interface between the 53% and 70% layers. Presence of the protein of interest was confirmed by immunoblot. To load protein into liposomes, inclusion bodies were solubilized in 6 M urea before overnight dialysis in egg yolk phospholipids dispersed in 1X potassium phosphate buffer. The dialyzed mixture was sonicated to generate the final proteoliposomes and protein concentration was determined by Bradford assay.

Determination of Heme by Reverse phase- High Pressure Liquid Chromatography

Preparation of samples includes purification by centrifugation and adjustment of pH as previously described. HPLC separation is then performed on C18 columns using a gradient mobile phase system (e.g., gradient A, methanol; gradient B, 0.05 mM monobasic sodium phosphate, pH 3.5) at 30–40 °C. By comparing the chromatograms of the sample and the standard used for calibration, the concentration can be calculated by integration of the peak areas. Labile heme is detected at 405 nm by RP-HPLC [16].

Analysis of PPIX Fluorescence in whole BY4741 cells

Protoporphyrin IX (PPIX) was diluted 1:1000 in pure methanol and the fluorescence intensity was measured using an excitation of 405 nm and emission of 633 nm (slit widths were set to 5 nm). Whole cell samples treated with exogenous copper or iron were lysed by centrifugation and resuspended in pure methanol for analysis. Fluorescence intensity was measured using a PerkinElmer Life Sciences LS55 spectrofluorometer. The spectra were plotted as a means of wavelength absorbance and intensity in Excel.

Statistical Methodology

ANOVA

A one-way analysis of variance (ANOVA) was used to determine whether there were any significant differences between the means of three or more independent (unrelated) groups. In all ANOVAs shown the experimental conditions were varying metal concentrations (copper or iron) with or without the addition of heme biosynthesis inhibitor, succinylacetone. Statistical significance of variance between the means of the populations in question for each experiment were measured using the p-value. P values <0.05 were taken as indications of strong evidence against the null hypothesis (H_0). Where H_0 is $\mu_{control} = \mu_{experimental}$ and there is no difference in means.

Miscellaneous methods

Succinlyacetone (4,6-dioxo-heptanoic acid) was purchased from Sigma-Aldrich (stock keeping unit no. D1415). Quantification of spot intensities in serial dilution growth tests were performed using IMAGEJ software [17]. Images were converted to grayscale then to binary using the following method: Process-Binary-Make binary. The rectangular selection tool was used to specify the area of interest and measured. All growth curves were performed using a Cytation 5 Biotek Multimode microplate reader.

.

Results

Yeast experiences a heme defect related to exogenous copper

To investigate the potential role of copper in heme synthesis we cultured cells in increasing concentration of copper and assayed for heme levels using a HPLC assay. In the medium supplemented with increasing copper concentration, we saw an increase of intracellular copper (2+/- 0.5 ng/µg S increased to 13+/- 3 ng/µg S for any medium concentration greater than 1 mM to 2.4 mM (data not shown)). This resulted in a dose dependent decrease in total heme (Figure 3.2C). This was independent of decreases in cellular iron concentrations. As iron did not change, we investigated if the copper induced defect was due to porphyrin synthesis defect, we assayed cells cultured in copper or the heme biosynthesis inhibitor succinyl-acetone (SA). SA resulted in a decrease in total heme without affecting total cellular iron and succinyl-acetone and copper were additive suggesting they disrupted different parts of the heme synthesis pathway (Figure 3.2B). To further investigate the impact of copper on heme synthesis, we assayed the effects of exogenous copper over a range of concentrations.

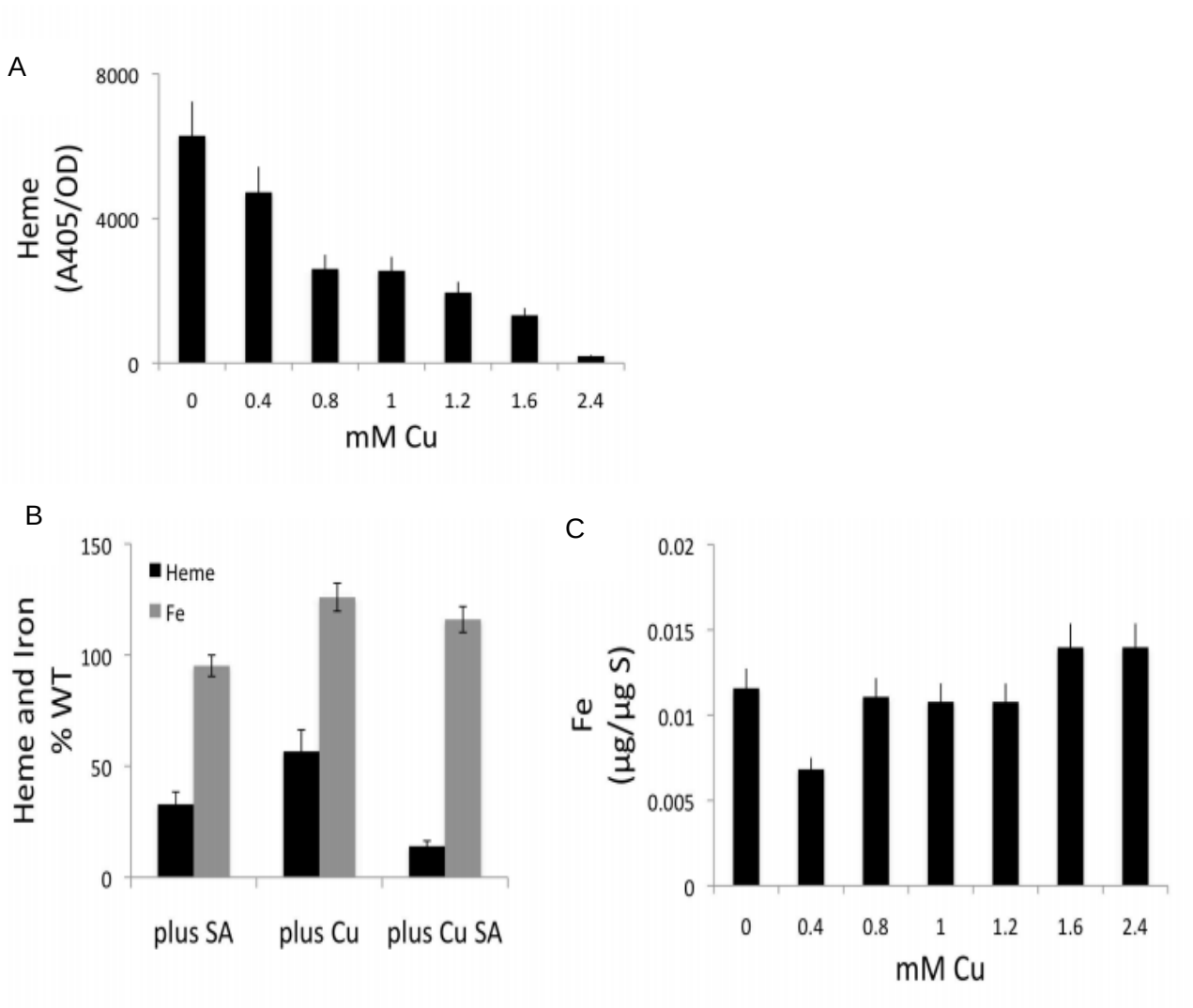

Figure 3.2. Heme analysis of whole cells

A) Wild-type yeast cells cultured in YP media supplemented with 1% sterile, filtered glucose and increasing concentrations of $CuSO_4$ and heme quantified relative to optical density. n=3 B) Heme and total cellular Fe in wild-type cells grown in 0.4 µM succinyl-acetone, 0.5 mM $CuSO_4$ or 0.4 µM succinyl-acetone plus 0.5 mM $CuSO_4$ as a percentage of maximum heme and Fe wild-type cells grown in YPD. n=3 C) Whole cell Fe concentrations from the cultures in B. n=3

Additive defect of succinylacetone is specific to copper when compared to iron

To further test the copper induced phenotype, we did a serial dilution growth test to compare growth in WT BY4741 yeast cells treated with varying concentrations of iron and copper with or without added SA. In WT BY4741 cells the growth defect phenotype is more pronounced when treated with high copper (Figure 3.3B). The defect is additive when SA is included in the media (Figure 3.3B). When treated with iron there is decreased growth as exogenous metal concentrations increase but the defect is not increased when succinyl acetone is added in comparison to cultures treated with copper and copper plus SA (Figure 3.3C). The scanned images of experiments were quantified, and the average of these images is shown (Figure 3.3A). Taken together, we show a copper specific growth defect that is additive in the presence of SA when compared to equal concentrations of exogenous iron.

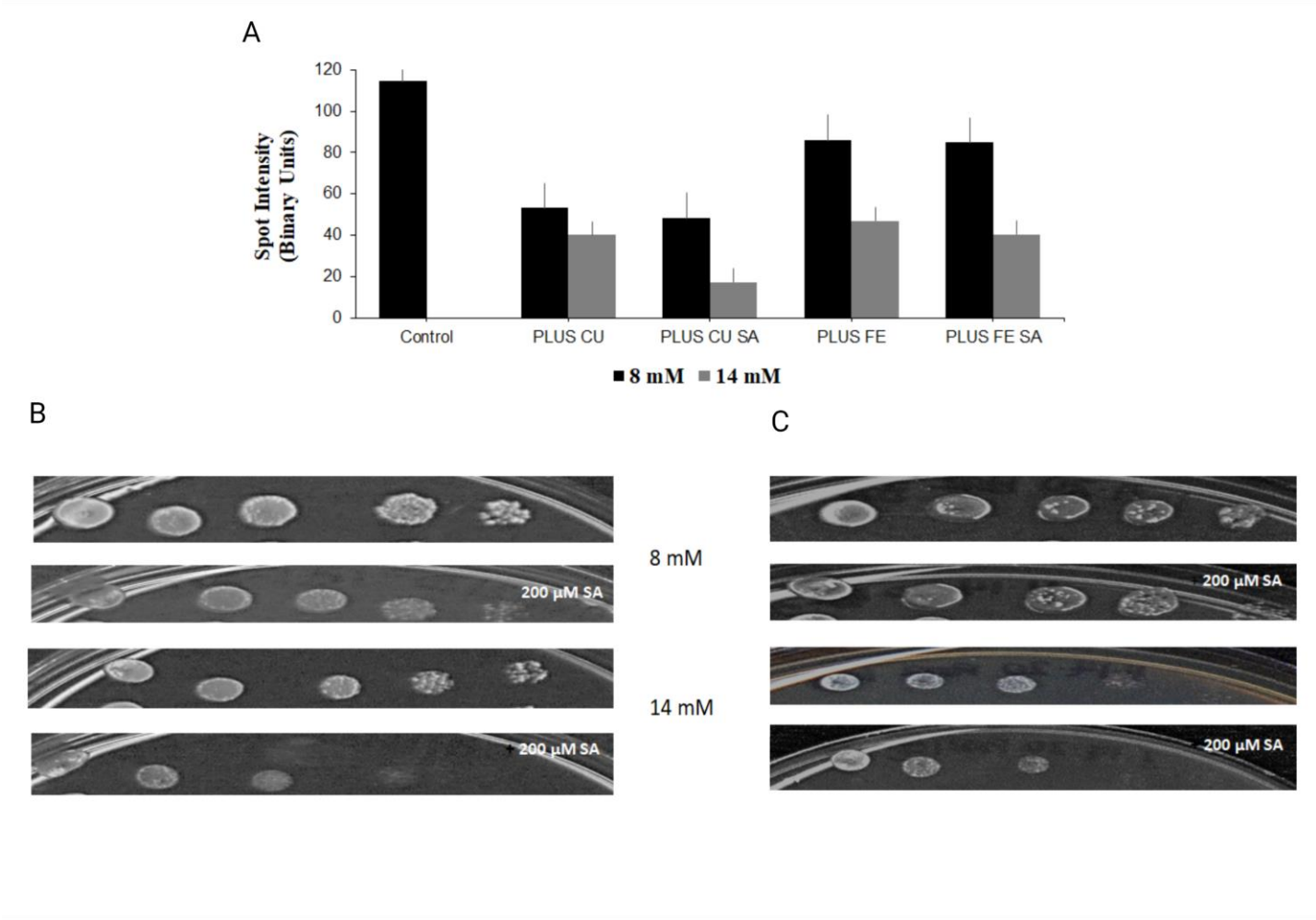

Figure 3.3 Copper specific growth phenotypes in WT BY4741

A) IMAGEJ was used to convert images and quantify spot intensity of serial dilutions of BY4741 grown on YPD agar with glucose as a carbon source. Cells were grown in the presence of the exogenous copper, iron with or without the combination of heme biosynthesis inhibitor succinylacetone (SA). The average of 3 separate experiments are pictured in panel A. Error bars pictured represent the standard error. B) Pictured serial dilutions from the graph mentioned above of BY4741 cells grown in the presence of 8 mM and 14 mM added copper +/- 200 µM SA. C) Pictured serial dilutions from the graph mentioned above of BY4741 cells grown in the presence of 8 mM and 14 mM added iron +/- 200 µM SA. A p-value of 8.37E-10 was obtained from a one-way ANOVA.

Heme defect is not recovered with a supplement of oleic acid, ergosterol and methionine (TEM) in media

To investigate possible mechanisms of disruption of the heme biogenesis pathway we attempted to alleviate the phenotypic defect by supplementing medium with oleic acid, ergosterol and methionine (abbreviated as TEM due to oleic acid being supplied as Tween 80). Copper dependent phenotypes observed for WT yeast were exaggerated by the addition of supplemented TEM media (Figure 3.4) rather than being reversed which would have suggested that the copper toxicity was linked to the heme defect. To further confirm the growth defect, we performed a yeast growth curve. The growth curve confirmed that the addition of TEM to copper containing media inhibited the growth of yeast (Figure 3.4)

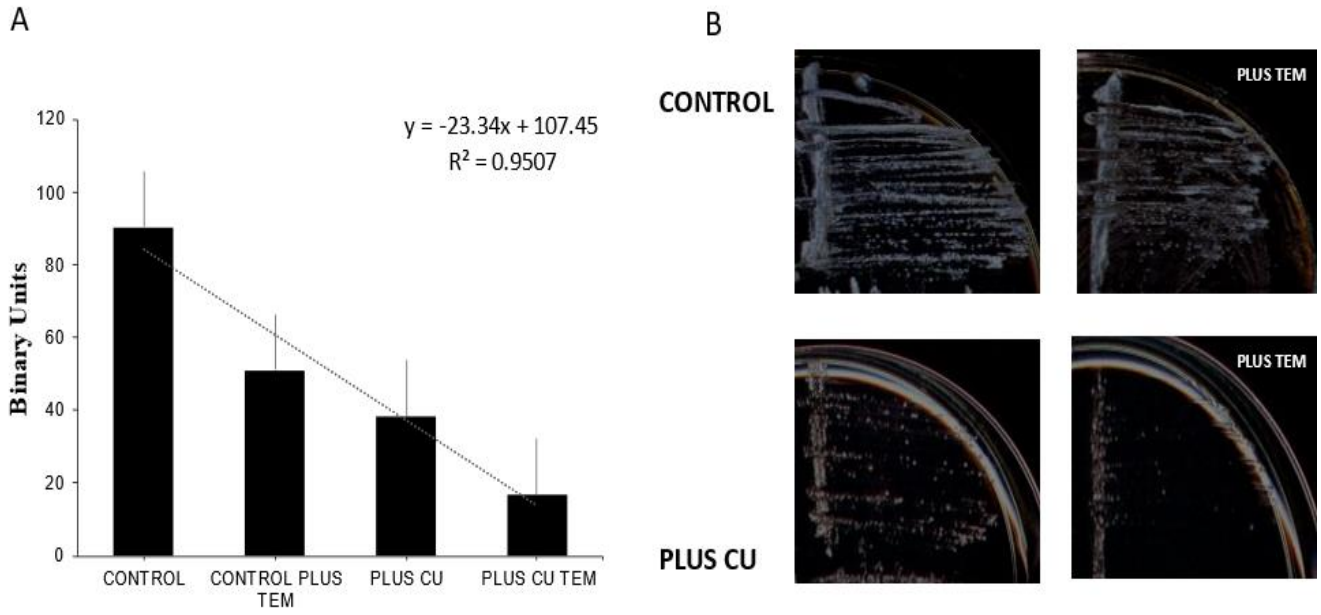

Figure 3.4 WT BY4741 growth defect in response to exogenous oleic acid (Tween 80), methionine and ergosterol (TEM)

Quantification of colony growth of copper and/or TEM treated cells in *S. cerevisiae.* A) Binary unit quantification of quadrant streaked YPD agar with added TEM supplement and/or added exogenous copper to the agar. Conversions of images were done using IMAGE J software, streaking for isolation in the same conditions was performed three separate times, the quantification above is representing one biological repeat of these experiments. For statistical purposes, a line of best fit was generated. Error bars pictured represent standard error. B) Scanned images of conditions quantified in A. The end OD compared across concentrations is lower in TEM supplemented groups (Figure 3.4A). When compared to lower concentrations of copper sulfate, populations treated with higher concentrations reach stationary phase quicker over an 18hr period (Figure 3.4B and Figure 3.4C). New cell formation in both groups is stunted by the addition of TEM media to the well.

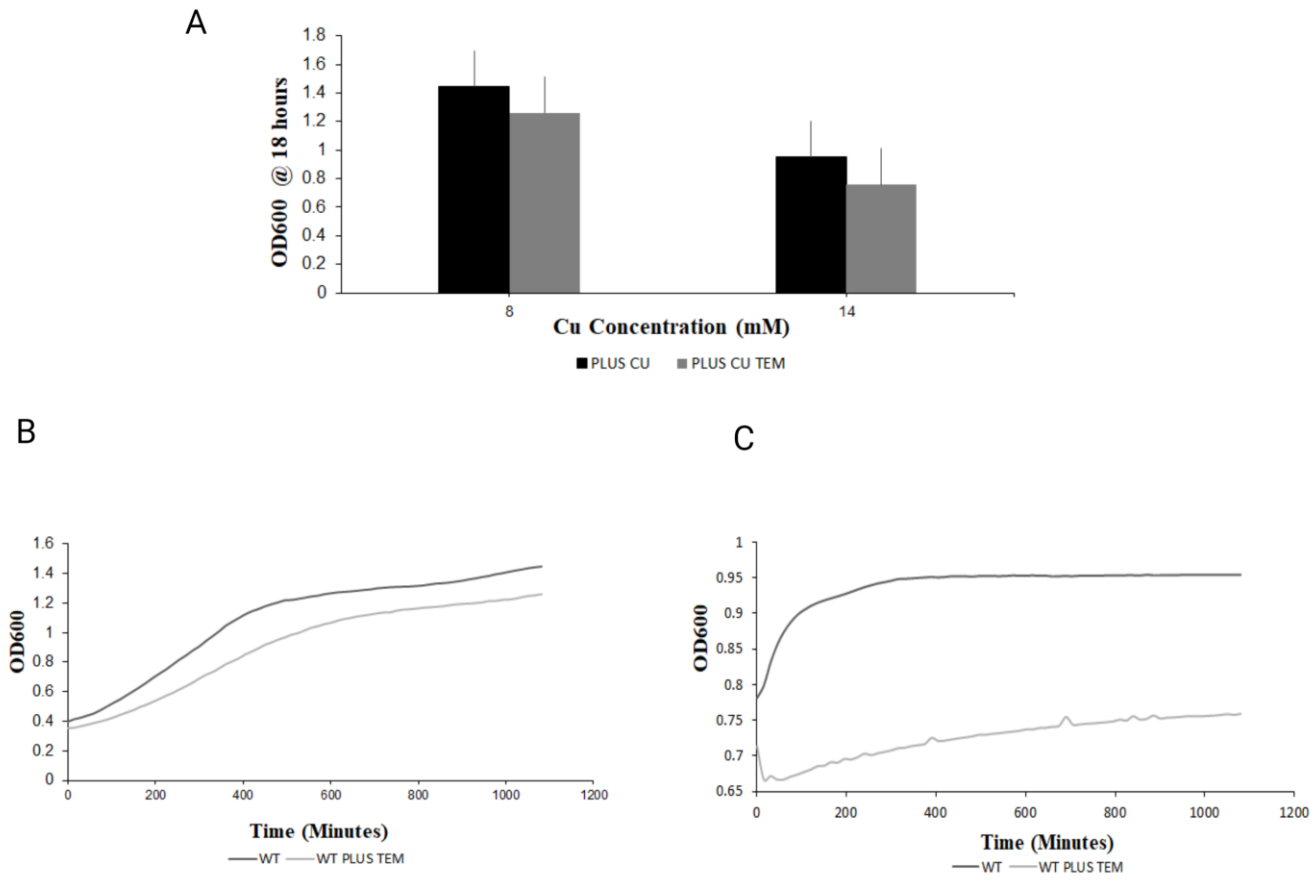

Figure 3.5 Growth curve of WT BY4741 yeast treated with a supplement of oleic acid, ergosterol and methionine (TEM) in media

Growth rate curve of *Saccharomyces cerevisiae* in response to supplemented copper and/or TEM A) Bar graph quantification of averages from the technical repeats of this experiment. The end value OD600 of the growth curve was taken and averaged amongst separate experiments. Error bars pictured represent the standard error. B) Growth curve over 18 hours of *S. cerevisiae* cultures treated with 8 mM of CuSO4 compared to cultures treated 8 mM of CuSO4 plus TEM. C) Growth curve over 18 hours of *S. cerevisiae* cultures treated with 14 mM of CuSO4 and 14 mM of CuSO4 plus TEM.

ATX, CCC2 and GSH1 mutants show similar additive copper and succinyl acetone growth defect with WT yeast

To test whether the heme defect is related to commonly known copper transport proteins such as the ATOX1-CCC2 complex or GSH, we performed comparative growth tests in WT BY4741, *ccc2Δ*, *atx1Δ*, and *gsh1Δ* **c**ells treated with varying concentrations of metals with or without added SA. In WT BY4741 cells the growth defect phenotype is more pronounced when treated with high copper (Figure 3.3C). The defect is additive when SA is added (Figure 3.3B). When treated with copper there is less growth as exogenous metal concentrations increase but this defect is not pronounced when SA is added (Figure 3.6B and Figure 3.6C). The average of the measurements is plotted in bar graphs (Figure 3.6A). Taken together, we cannot report a phenotypic implication for the mentioned proteins in the copper induced heme defect in *S. cerevisiae*.

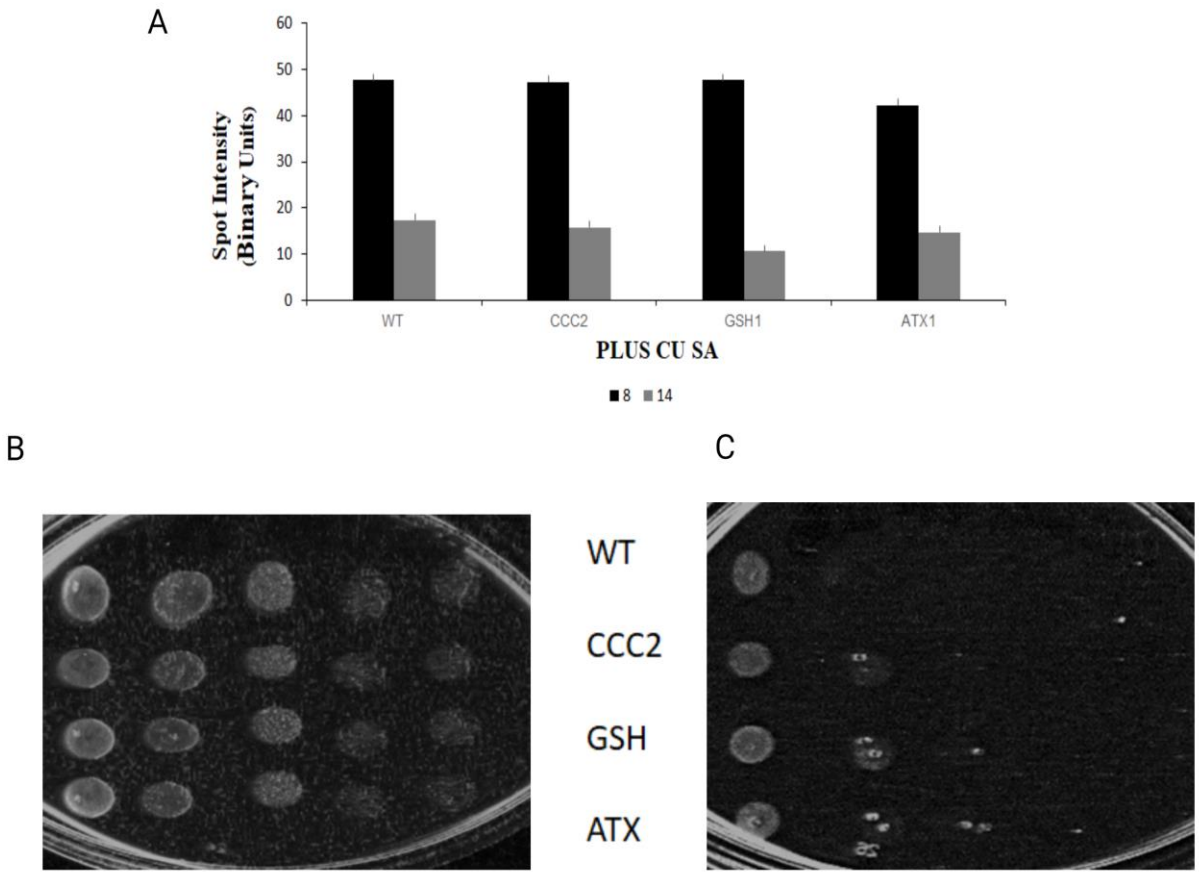

Figure 3.6 Serial dilution growth test of WT BY4741

Serial dilutions of WT BY4741 yeast in growth conditions with exogenous copper and added succinylacetone (SA). Dilutions were performed ten-fold and are pictured as 1, 1:10, 1:100. 1:1000, respectively. A) Spot intensity quantification prepared using IMAGEJ software plates were scanned and converted to binary units. Spot intensity of corresponding serial dilutions were measured and averaged, and error bars pictured represent the standard error B) Pictured Serial dilutions of WT yeast on YPD agar plates with 8 mM plus 200 µM of exogenous copper added to the media C) Pictured Serial dilutions of WT yeast on YPD agar plates with 14 mM of exogenous copper plus 200 µM of SA added to the media A p-value of 0.997254 was obtained from a one-way ANOVA. n=3 for each group.

Excess copper interferes with the availability of PPIX

To indirectly assess ferrochelatase (FCH) activity in *S. cerevisiae* after treatment with exogenous metals the yeast cells were lysed, and protein removed by the addition of methanol. Protoporphyrin IX (PPIX) levels of samples were measured by fluorescence spectroscopy. Whole cell samples were treated with exogenous copper or iron and were lysed by centrifugation and resuspended in pure methanol for analysis. PPIX in the lysate was excited by red light (approximately 635 nm), the signal was defined as the intensity of the spectrally fit PPIX component present in the measured spectrum.

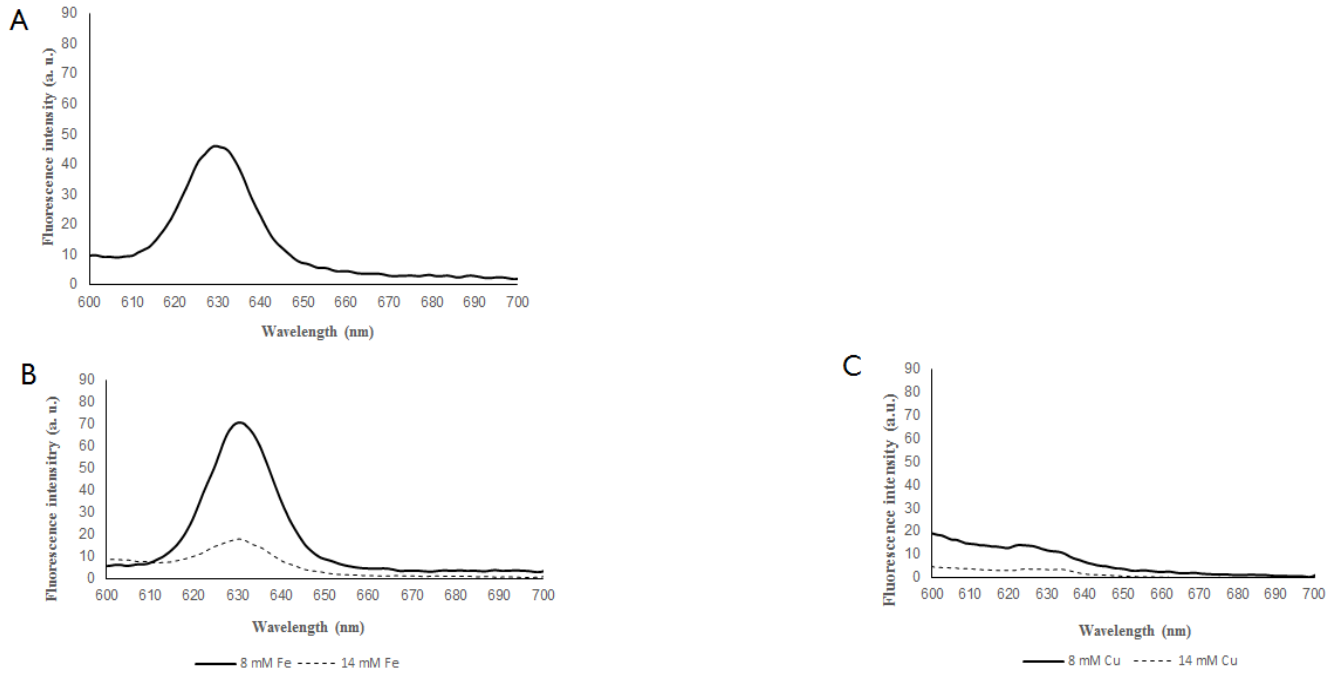

Figure 3.7 Fluorescence spectroscopy of PPIX in WT BY4741

PPIX fluorescence intensity in cell lysates of *S. cerevisiae*. PPIX in the lysate was excited by red light (approximately 635 nm), the signal was defined as the intensity of the spectrally fit PPIX component present in the measured spectrum. PPIX fluorescence in methanol has an emission of 630±5 nm. A) The fluorescence spectra of PPIX solution diluted in methanol 1:1000. B) The fluorescence spectra of PPIX in lysate of *S. cerevisiae* extracted in pure methanol treated with 8 and 14 mM $FeSO_4$, respectively. C) The fluorescence spectra of PPIX in lysate of *S. cerevisiae* in pure methanol treated with 8 and 14 mM CuSO4, respectively.

Copper-induced heme defect was lost upon deletion of MRS3

Due to the potential connection of iron and copper in mitochondria because of the overlap of substrate specificity of Mrs3, we assayed the effects of exogenous copper on heme levels. Heme levels in wild type (WT) were higher than in mrs*3*Δ cells presumably due to lower iron availability. To rescue this defect, we supplemented the medium exogenous iron. This resulted in increased heme synthesis in both WT and *mrs3*Δ demonstrating the iron is limiting even in WT cells. As a control experiment, we added supplemental copper and surprisingly it induced a heme deficit in WT cells like levels of *mrs3*Δ cells in non-supplemented media (Figure 3.8). The copper-induced heme defect was lost upon deletion of *MRS3* (Figure 3.8). Mammalian homologues or Mrs3/Mrs4 known as mitoferrin have shown the ability to transport multiple metals including copper, therefore we assayed the effects of exogenous copper on heme levels in multiple mutants. In addition, we assayed *mrs4*Δ, and *pic2*Δ cells grown in fermentable media with and without 0.5 mM FeSO4 or 1 mM $CuSO_4$. The effect of copper on heme synthesis was lost when *MRS3* was deleted.

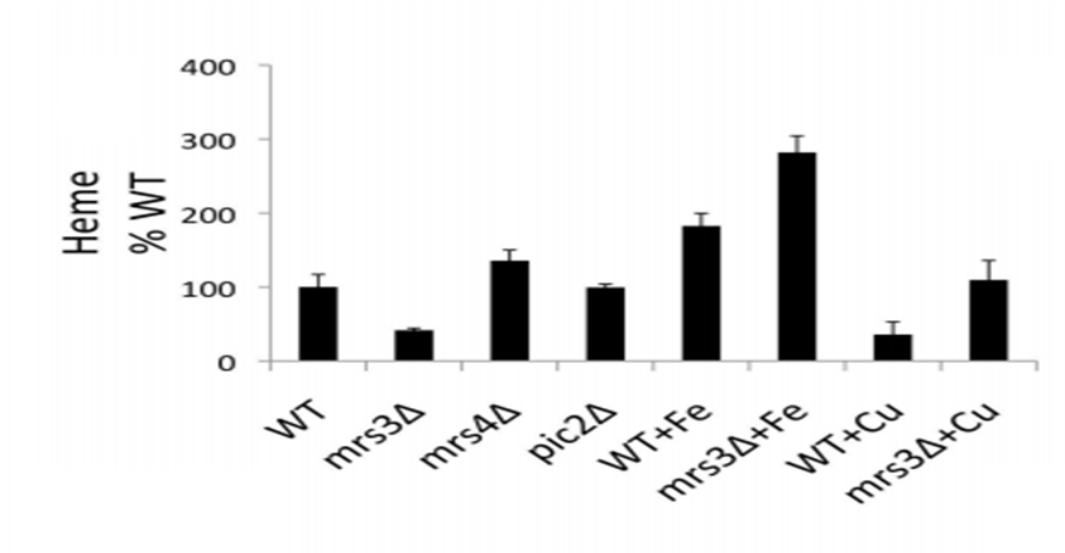

Figure 3.8 Heme analysis of whole cells

Graphed is heme quantified by area under the curve of absorbance at 405 nm after reverse phase chromatography and converted to percentage of maximum heme from wild-type BY4741 yeast. Heme levels in wild-type and mrs3Δ cells increased with the addition of exogenous Fe while supplemental copper caused a heme deficit in WT cells and mrs3Δ cells in non-supplemented media the copper-induced heme defect was lost upon deletion of MRS3. (n=3 for each example, error bars are standard deviation)

Results of Analysis of Variance (ANOVA)/ Multiple Comparisons Test

To determine if there were significant differences between the groups of each experiment a one-way ANOVA was used. The p- value is used to determine statistical significance. If $P < 0.05$ then sample results are usually deemed significant at a statistically important level and thus the null hypothesis is rejected. For the analysis below the dependent variable is the growth of yeast cells and the independent variable is copper/SA treatment. The null hypothesis is $Total_{control} = Total_{experimental,}$ where total is the number of yeast colonies grown. If the p-value indicated that the data was statistically significant, pairwise post-hoc testing was performed to determine whether there was a difference between all possible pairs using studentized range distribution [18].

Table 3.1 Copper versus iron (plus succinylacetone) ANOVA results

Source of Variation	SS	df	MS	F	**P-value**	F crit
Between Groups	21651.51	8	2706.439	38.84079	**8.37E-10**	2.510158
Within Groups	1254.246	18	69.68033			
Total	22905.76	26				

The p-value is less than the assigned significance level 0.05. Thus, we reject the null hypothesis and state that the result is statistically significant.

Table 3.2 Tukey's multiple comparison test (Copper, Iron and SA)

Tukey's multiple comparisons test	Mean Diff.	95.00% CI of diff.	Below threshold?	Summary	Adjusted P Value	
Control vs. 8 Cu	61.65	39.06 to 84.24	Yes	****	<0.0001	A-B
Control vs. 8 Cu plus SA	66.65	44.06 to 89.24	Yes	****	<0.0001	A-C
Control vs. 8 Fe	28.7	6.113 to 51.29	Yes	**	0.0073	A-D
Control vs. 8 Fe plus SA	30.65	8.061 to 53.24	Yes	**	0.0039	A-E
Control vs. 14 Cu	74.65	52.06 to 97.24	Yes	****	<0.0001	A-F
Control vs. 14 Cu plus SA	97.3	74.71 to 119.9	Yes	****	<0.0001	A-G
Control vs. 14 Fe	68.65	46.06 to 91.24	Yes	****	<0.0001	A-H
Control vs. 14 Fe plus SA	74.65	52.06 to 97.24	Yes	****	<0.0001	A-I
8 Cu vs. 8 Cu plus SA	5	-17.59 to 27.59	No	ns	0.9963	B-C
8 Cu vs. 8 Fe	-32.95	-55.54 to -10.36	Yes	**	0.0019	B-D
8 Cu vs. 8 Fe plus SA	-31	-53.59 to -8.410	Yes	**	0.0035	B-E
8 Cu vs. 14 Cu	13	-9.590 to 35.59	No	ns	0.5519	B-F
8 Cu vs. 14 Cu plus SA	35.65	13.06 to 58.24	Yes	***	0.0008	B-G
8 Cu vs. 14 Fe	7	-15.59 to 29.59	No	ns	0.9692	B-H
8 Cu vs. 14 Fe plus SA	13	-9.590 to 35.59	No	ns	0.5519	B-I
8 Cu plus SA vs. 8 Fe	-37.95	-60.54 to -15.36	Yes	***	0.0004	C-D
8 Cu plus SA vs. 8 Fe plus SA	-36	-58.59 to -13.41	Yes	***	0.0007	C-E
8 Cu plus SA vs. 14 Cu	8	-14.59 to 30.59	No	ns	0.9359	C-F
8 Cu plus SA vs. 14 Cu plus SA	30.65	8.056 to 53.24	Yes	**	0.0039	C-G
8 Cu plus SA vs. 14 Fe	2	-20.59 to 24.59	No	ns	>0.9999	C-H
8 Cu plus SA vs. 14 Fe plus SA	8	-14.59 to 30.59	No	ns	0.9359	C-I
8 Fe vs. 8 Fe plus SA	1.948	-20.64 to 24.54	No	ns	>0.9999	D-E
8 Fe vs. 14 Cu	45.95	23.36 to 68.54	Yes	****	<0.0001	D-F
8 Fe vs. 14 Cu plus SA	68.59	46.00 to 91.18	Yes	****	<0.0001	D-G
8 Fe vs. 14 Fe	39.95	17.36 to 62.54	Yes	***	0.0002	D-H
8 Fe vs. 14 Fe plus SA	45.95	23.36 to 68.54	Yes	****	<0.0001	D-I
8 Fe plus SA vs. 14 Cu	44	21.41 to 66.59	Yes	****	<0.0001	E-F
8 Fe plus SA vs. 14 Cu plus SA	66.65	44.06 to 89.24	Yes	****	<0.0001	E-G
8 Fe plus SA vs. 14 Fe	38	15.41 to 60.59	Yes	***	0.0004	E-H
8 Fe plus SA vs. 14 Fe plus SA	44	21.41 to 66.59	Yes	****	<0.0001	E-I
14 Cu vs. 14 Cu plus SA	22.65	0.05648 to 45.24	Yes	*	0.0492	F-G
14 Cu vs. 14 Fe	-6	-28.59 to 16.59	No	ns	0.9878	F-H
14 Cu vs. 14 Fe plus SA	0	-22.59 to 22.59	No	ns	>0.9999	F-I
14 Cu plus SA vs. 14 Fe	-28.65	-51.24 to -6.056	Yes	**	0.0074	G-H
14 Cu plus SA vs. 14 Fe plus SA	-22.65	-45.24 to -0.05648	Yes	*	0.0492	G-I
14 Fe vs. 14 Fe plus SA	6	-16.59 to 28.59	No	ns	0.9878	H-I

A Tukey-Kramer Post-Hoc test was used to compare the population's means of *S. cerevisiae* growth in response to added copper, iron, or SA to growth medium. Absolute mean difference between each group was found using the averages listed in the ANOVA output, studentized Range Q Table was used to find the Q value and lastly absolute mean difference was measured between each group to the critical Q value. If the absolute mean difference is greater than the Q critical value, then the difference between the group averages is statistically significant. For this test we found that the difference in means in the following groups were not statistically significant: B and C, B and F, Band I, C and D, C and H, C and I, D and E, F and H, F and I, and H and I.

Table 3.3 Serial dilutions comparing ATX, GSH, and CCC2 mutant ANOVA results

Source of Variation	SS	df	MS	F	**P-value**	F crit
Between Groups	21.91846	3	7.306154	0.014411	**0.997254**	6.591382
Within Groups	2028.002	4	507.0005			
Total	2049.92	7				

The p-value is greater than the assigned significance level 0.05. Thus, we fail to reject the null hypothesis and state that the result is statistically nonsignificant (n.s.).

Discussion

In this study, an additive defect of porphyrin inhibition and copper accumulation is observed in yeast. In 1 mM SA there is a significant inhibition of ALA dehydratase activity [24]. In this study a concentration of 200 micromolar concentration was used in YPD medium and YPD agar plates, yet there was still a pronounced growth defect. The copper related heme defect was not alleviated by supplementing the medium with the products of heme requiring pathways (oleic acid, ergosterol or methionine). These additives rescue mutants in *HEM1*, *HEM2* and *HEM3* had a growth requirement for methionine supplemented with ergosterol and Tween 80 on synthetic medium due to a lack of efficient sulfite reductases [19]. *HEM1* gene encodes delta-aminolevulinic acid synthase, deletion of these genes will result in decreased transcription of genes associated with copper regulons and iron regulons but not zinc reglons [2]. *HEM2* encodes a cytoplasmic zinc-dependent enzyme that is involved in the second step of heme biosynthesis [20]. *HEM3* encodes an enzyme that catalyzes the conversion of 4-porphobilinogen to hydroxymethylbilane which is the third step in heme biosynthesis [19,21]. The additive growth defect in the presence of TEM media in the presence of copper suggests that copper does not disrupt heme biosynthesis at these mentioned steps. Another potential known area of interest for heme deficiencies in this study are blocks in FCH function. From the results of this study, we cannot definitively draw conclusions on the activity of FCH during times of copper accumulation. However, some assumed functions seem to take place during these times due to decreased levels of PPIX detected in WT yeast cells treated with high levels of copper. Further experiments testing cells in these conditions with heme protein specific mutations in the presence of absence of heme and PPIX are needed to draw these conclusions. Taking these findings into account it seems that heme deficiency during copper overload cannot be solely attributed to

related protein dysfunction but rather substrate inhibition perhaps due to decreased iron in mitochondria.

Heme biogenesis disruption does not seem to be reliant on metallochaperone proteins such as Atx1, which is required for delivery of copper to Ccc2 for eventual incorporation into the multicopper oxidase Fet3. The delivery of copper to ATPase transporters is an important mechanism for subsequent insertion of copper into ceruloplasmin in mammals which is required for proper iron metabolism [23]. However, *atx1*Δ and *ccc2*Δ mutants do not show a remarkable growth difference when treated with copper and SA. From this we can conclude that when related to heme biosynthesis there is no specific defect in the Atx1 and Ccc2 transfer process as it is related to copper shuttling or iron metabolism.

Unlike other eukaryotes, plants and fungi do not synthesize cytosolic ferritin which is a conserved iron storage and iron detoxification protein. As a mechanism for storing iron and detoxification, plants and fungi store their iron and many other molecules in the vacuole [25]. Recent studies have examined how the deletion of *MRS3* and *MRS4* affect cellular metabolism in mechanisms not related to mitochondria. Findings of the studies report that deletion of these genes leads to activation of the vacuolar iron transporter Ccc1 and a consequent depletion of cytosolic iron [26]. However, considering our findings, we propose that deletion of mitochondrial proteins can alter vacuolar metal homeostasis and activation of vacuolar metal transporters. All together this leads to a disruption in mitochondrial processes such as heme biogenesis. In terms of mitochondrial-vacuolar interactions disruption of heme biogenesis may arise from the depletion of cytosolic iron when iron is transported to the vacuole is *S. cerevisiae*, making it easier for copper binding to Mrs3. Vacuolar iron transport is increased in *Δmrs3Δmrs4* cells, resulting in decreased cytosolic iron and activation of the iron-sensing transcription factor

Aft1. Activation of Aft1 leads to increased expression of the high affinity iron transport system and increased iron uptake. Deletion of *CCC1* in *Δmrs3Δmrs4* cells restores cellular and mitochondrial iron homeostasis to near normal levels. *Δmrs3Δmrs4* cells also show increased resistance to cobalt but decreased resistance to copper and cadmium. These phenotypes are also corrected by deletion of *CCC1* in *Δmrs3Δmrs4* cells. Decreased copper resistance in *Δmrs3Δmrs4* cells results from activation of Aft1 by Ccc1-mediated iron depletion, as deletion of *CCC1* or *AFT1* in *Δmrs3Δmrs4* cells restores copper resistance [27,28]. These results suggest that deletion of mitochondrial proteins can alter vacuolar metal homeostasis. The data also indicate that increased expression of the AFT1-regulated gene(s) can disrupt copper homeostasis.

In conclusion, we report phenotypic and biochemical evidence for a copper dependent heme defect in *S. cerevisiae*. *MRS3* has been shown to have copper transporting abilities and mediates iron transport. The disruption of the heme biogenesis pathway is likely not due to mishaps in the first three steps of heme biogenesis. We did not address whether the insertion of ferrous iron into PPIX by ferrochelatase is affected during copper accumulation. A better understanding of the molecule events occurring in the heme biosynthesis pathway such as how cells make iron available, will improve the approach to biochemical assays and transport assays so that we can better understand metal homeostasis in mitochondria.

References

1. O'Reilly, S., Pollycove, M., Bank, W. (1968) Iron Metabolism in Wilson's disease. Kinetic studies with iron. *Neurology* 18, 634-644.
2. Crisp, R. J., Kaplan, J., (2003) Inhibition of Heme Biosynthesis Prevents Transcription of Iron Uptake Genes in Yeast. *Metabolism and Bioenergetics.* 278, 45499-45506.
3. Puige, S.,Thiele D.J. Molecular mechanisms of copper uptake and distribution. (2006) *Biochimica et Biophysica Acta (BBA) - Molecular Cell Research* 1763, 759-772.
4. Huffman, D.L., O'Halloran, T.V. (2001) Function,structure, and mechanism of intracellular copper trafficking proteins. *Annu. Rev. Biochem.* 70, 677-701.
5. Lin, S.J., Pufahl, R. A., Dancis A., O'Halloran T. V., Culotta, V. C. (1997) A role for the Saccharomyces cerevisiae ATX1 gene in copper trafficking and iron transport. *J. Biol. Chem* 272, 9215-9220.
6. Klomp, L.W.J, Lin S-J., Yuan D. S., Klausner R. D., Culotta V. C., Gitlin J. D. (1997) Identification and functional expression of HAH1, a novel human gene involved in copper homeostasis. *J. Biol. Chem* 272, 9221-9226.
7. O'Halloran, T.V., Culotta V. C. (2000) Metallochaperones, an intracellular shuttle service for metal ions. *J. Biol. Chem* 275, 25057-25060.
8. Froschauer, E. M., Wiesenberger, G. (2009) The yeast mitochondrial carrier proteins Mrs3p/Mrs4p mediate iron transport acroos the inner mitochondrial membrane. *Biochimica et Biophysica Acta (BBA) - Biomembranes* 1788, 1044-1050.
9. Palmieri, F., Agrimi, G., Blanco, E., Castegna, A., Di Noia, M. A., Iacobazzi, V., Lasorsa F. M., Marobbio C. M. T., Palmieri L., Scarcia P., Todisco S., Vozza A., Walker J. (2006) Identification of mitochondrial carriers in *Saccharomyces cerevisiae* by transport assay of reconstituted recombinant proteins. *Biochim. Biophys. Acta* 1757, 1249-1262.
10. Foury, F., Roganti T. (2002) Deletion of the mitochondrial carrier genes MRS3 and MRS4 suppresses mitochondrial iron accumulation in a yeast frataxin-deficient strain.. *J. Biol. Chem.* 277, 24475-24483.
11. Mühlenhoff, U., Stadler J. A., Richhardt N., Seubert A., Eickhorst T., Schweyen R. J., Lill R., Wiesenberger G. (2003) A specific role of the yeast mitochondrial carriers Mrs3/4p in mitochondrial iron acquisition under iron-limiting conditions. *J. Biol. Chem* 278, 40612-40620.
12. Zhang, Y., Lyver, E. R., Knight, S. A. B., Pain D., Lesuisse E. (2006) Mrs3p, Mrs4p, and frataxin provide iron for Fe–S cluster synthesis in mitochondria. *J. Biol. Chem* 281, 22493-22505.
13. Layer, G., Reichelt, J., Jahn, D., Heinz D. W. (2010) Structure and function of enzymes in heme biosynthesis. *Protein Science* 19, 1137-1161.
14. Hunter, G. A., Sampson, M. P., Ferreira G. C. (2008) Metal Ion Substrate Inhibition of Ferrochelatase. *J. Biol. Chem* 29, 23685-23691.
15. Palmieri, L., Runswick, M. J., Fiermonte, G., Walker J. E., Palmieri, F. (2000) Yeast mitochondrial carriers: bacterial expression, biochemical identification and metabolic significance. *Journal of bioenergetics and biomembranes* 32, 67-77.
16. Woods, J. S., Simmonds, P. L. (2001) HPLC methods for analysis of porphyrins in biological media. *Curr. Protoc. Toxicol* 7, 8.91-8.9.17.

17. Rasband, W.S. (1997-2016) *Image J. U.S. National Institute of* Health, Bethesda, Maryland, USA.
18. Dubitzky, W., Wolkenhauer, O., Cho, K. H., Yokota, H. (2013) Tukey–Kramer Method. *Encyclopedia of Systems Biology.*
19. Ponka, P. (1999) Cell biology of heme. *Am. J. Med. Sci* 318, 241-256.
20. Gollub, E. G., Liu, K-P., Dayan J., Aldersberg M., Sprinson D. B. (1977) Yeast mutants deficient in heme biosynthesis and a heme mutant additionally blocked in cyclization of 2,3-oxidosqualene. *J. Biol. Chem* 9, 2846-2854.
21. Myers, A. M., Crivellone M. D., Koerner T. J., Tzagoloff A. (1987) Characterization of the yeast HEM2 gene and transcriptional regulation of COX5 and COR1 by heme. *J. Biol. Chem* 262, 16822-16829.
22. Keng, T., Larocque, R. (1992) Structure and regulation of yeast HEM3, the gene for porphobilinogen deaminase. *Molecular and General Genetics MGG* 234, 233-243.
23. Bertini, I., Gray, H. B., Stiefel, E.I., Valentine, J. S. (2006) Biological Inorganic Chemistry. Structure and Reactivity. *Angewandte Chemie International Edition* 46, 8741-8742.
24. Vest, K. E., Leary, S. C., Winge, D. R., Cobine, P. A. (2013) Copper import into the mitochondrial matrix in Saccharomyces cerevisiae is mediated by Pic2, a mitochondrial carrier family protein. *The Journal of biological chemistry*, 288, 23884–23892.
25. Ebert , P. S., Tschudy, D. P. (1979) Succinylacetone, a potent inhibitor of heme biosynthesis: Effect on cell growth, heme content and δ-aminolevulinic acid dehydratase activity of malignant murine erythroleukemia cells. *Biochemical and Biophysical Research Communications* 88, 1382-1390.
26. Raguzzi F., Lesuisse E., Crichton R. R. (1988) Iron storage in Saccharomyces cerevisiae. *FEBS Lett.* 231, 253-258.
27. Li, L., Murdock, G., Bagley, D., Jia, X., Ward, D. M., Kaplan, J. (2010) Genetic dissection of a mitochondria-vacuole signaling pathway in yeast reveals a link between chronic oxidative stress and vacuolar iron transport. *J. Biol. Chem.* 285, 10232–10242.
28. Li, L., Kaplan, J. (2004) A mitochondrial-vacuolar signaling pathway in yeast that affects iron and copper metabolism. *J. Biol. Chem.* 279, 33653-33661,

Chapter 4: Concluding Remarks

Copper and iron are essential for cellular processes and play an important factor in numerous vital cellular functions. Both metals are involved in many different cellular pathways including the electron transport chain, removal of reactive oxygen species, iron-sulfur biogenesis, and heme biogenesis. However, both metal's ability to gain and accept electrons allow them to be potentially harmful to cells in imbalance. Copper and iron have important roles in oxidative stress and enzymatic functions make them critical in mitochondria. Consequently, mitochondria are key organelles for transition metals. The relationship between mitochondrial metabolism and changing concentration of transition metals is a topic that leaves many questions unanswered.

There is a correlation between lowering glutathione levels and rising copper ion levels. GSH is the main target of copper ions during times of copper accumulation. One of the most studied GSH precursors is the amino acid cysteine. Copper-cysteine interactions play an important role in biological functions. Copper has a high affinity for binding with sites that are cysteine rich as does iron. This likeness can lead to overlapping of the systems that deal with each of the metals, respectively. A consequence of this overlap is a copper related heme defect in *S. cerevisiae*. Copper damage has long been reported but little evidence points to it being accredited to sulfhydryl groups in proteins or heme biogenesis.

Mrs3 is one of the many members of the mitochondrial carrier family (MCF). The MCF family is responsible for the flux of many compounds across the inner membrane of the mitochondria, including iron. Deletion of *MRS3*, however, also causes a copper-dependent heme defect in *S. cerevisiae* demonstrating an important overlap in import machinery. This competition for binding leads to decreased levels of heme. The exact pathway for how the heme

biogenesis pathway is disrupted is left to be answered. Observed decreased levels in PPIX, the precursor to heme, during times of accumulated copper allude to free copper possibly binding to FCH. Though FCH was not directly tested in this study, indirectly the function of the protein is not inhibited during times of copper accumulation. Other mutants such as Atx1 and Ccc2 do not seem to exhibit a significantly different growth phenotype related to heme biogenesis inhibition.

Here we can conclude that:

1) Cysteine and GSH are major players in copper redox, transportation and most importantly cell damage responses. Copper's affinity for them makes them key targets during times of copper overload in the cell and mitochondria. Cysteine rich proteins and thiolate proteins are key targets for copper-dependent damage in mitochondria.
2) Matrix copper transport is mediated by MCF member Mrs3 which can lead to a heme related defect in mitochondria under copper stress (Figure 4.2).
3) Mitochondrial damage observed in Wilson disease patients and several models of Wilson disease are probably attributable to glutathione oxidation and targeting, defects in iron-sulfur cluster biogenesis and/or heme biogenesis pathway disruption.

Further study is needed to understand the many factors that contribute to copper and iron dependent defect phenotypes. Growing knowledge of these factors and mitochondrial metal homeostasis are the right steps in understanding mitochondrial damage and diseases.

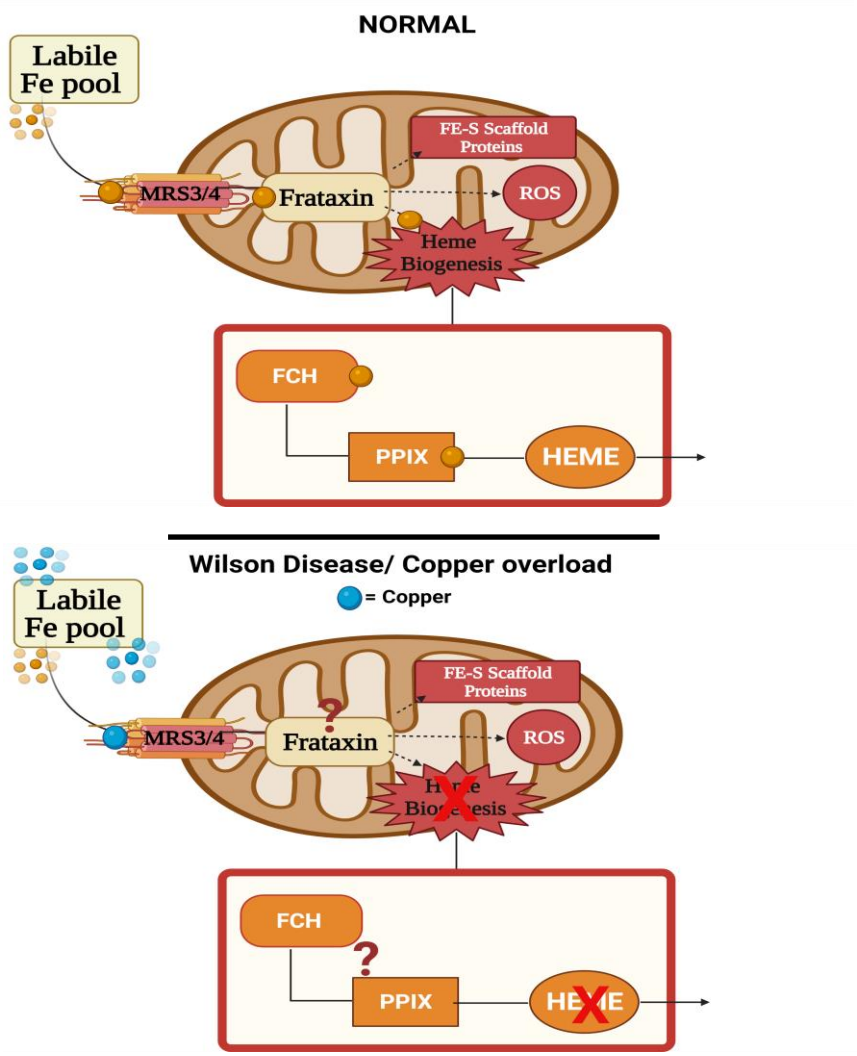

Figure 4.1 Copper dependent heme defect via MRS3

MRS3, a member of the MCF, has been identified for involvement in iron transport. When copper is present in high levels, it has potential to bind with transporters such as MRS3 and is then transported to the matrix. This copper then has potential to disrupt the heme synthesis pathway by possibly binding to FCH and/or PPIX. It also may contribute to damage of iron sulfur clusters which aid in protection against reactive oxygen species that arise during copper overload. Created with Biorender.com.